Mafic inputs into the rhyolitic magmatic system of the 2.08 Ma Huckleberry Ridge eruption, Yellowstone

Revision 1

Elliot J. Swallow[a]*, Colin J.N. Wilson[a], Bruce L.A. Charlier[a], John A. Gamble[a]

[a] School of Geography, Environment and Earth Sciences, Victoria University of Wellington, P.O. Box 600,Wellington 6140, New Zealand

Manuscript for: *American Mineralogist*

*Corresponding author. Email address: elliot.swallow@vuw.ac.nz

Always consult and cite the final, published document. See http:/www.minsocam.org or GeoscienceWorld

DOI: https://doi.org/10.2138/am-2018-6273

Abstract

The silicic (broadly dacitic to rhyolitic) magmatic systems that feed supereruptions show great diversity, but have in common a role for mafic (broadly basaltic to andesitic) magmas as drivers of the systems. Here we document the mafic component in the rhyolitic magmatic system of the 2.08 Ma Huckleberry Ridge Tuff (HRT, Yellowstone), and compare it to mafic materials erupted prior to and following the HRT eruption in the area within and immediately around its associated caldera. The HRT eruption generated initial fall deposits, then three ignimbrite members A, B and C, with further fall deposits locally separating B and C. A 'scoria' component was previously known from the upper B ignimbrite, but we additionally recognise juvenile mafic material as a sparse component in early A, locally abundant in upper A and sparsely in lower B. It has not been found in the C ignimbrite. In upper B the mafic material is vesicular, black to oxidised red-brown scoria, but at other sites is overwhelmingly non-vesicular, and sparsely porphyritic to aphyric. Despite their contrasting appearances and occurrences, the mafic components form a coherent compositional suite from 49.3-63.3 wt % SiO_2, with high alkalis (Na_2O+K_2O = 4.5-7.3 wt %), high P_2O_5 (0.52-1.80 wt %), and notably high concentrations of both high field strength and large-ion lithophile elements (e.g. Zr = 790-1830 ppm; Ba = 2650-3800 ppm). Coupled with the trace-element data, Sr-Nd-Pb isotopic systematics show influences from Archean age lower crust and lithospheric mantle modified by metasomatism during the late Cretaceous to Eocene, as previously proposed for extensive Eocene magmatism/volcanism around the Yellowstone area. The HRT mafic compositions contrast markedly with the Snake River Plain olivine tholeiites erupted before and after the HRT eruption, but are broadly similar in several respects to the generally small-volume Craters of the Moon-type mafic to

Always consult and cite the final, published document. See http:/www.minsocam.org or GeoscienceWorld

intermediate lavas erupted recently just west of the HRT caldera, as well as farther west in their type area. The combination of trace element and isotopic data on the HRT mafics are only consistent with an origin for their parental magma as melts from mantle enriched by high temperature and pressure melts, most likely from the underlying Farallon slab. Subsequent interaction of the HRT mafic magmas occurred with the Archean lower crust and lithospheric mantle, but not the highly radiogenic upper crust in this area. The close temporal and spatial relationships of the HRT mafic compositions and the preceding Snake River Plain olivine tholeiite eruptives suggest a high degree of spatial heterogeneity in the mantle beneath the Yellowstone area during the early (and subsequent) development of its modern magmatic system.

Keywords: Yellowstone, Huckleberry Ridge Tuff, Craters of the Moon, mafic magmas, magma genesis, mantle metasomatism

Introduction

Mafic magmas (in this context basaltic to andesitic in composition) are widely considered to exert a fundamental control on the generation and development of large-scale silicic (dacitic to rhyolitic) magmatic systems in the crust (e.g. Hildreth 1981; Bachmann and Bergantz 2008). Over the long-term, mafic magmas provide heat and mass that drive the development of the silicic system (e.g. Bindeman et al. 2008; Christiansen and McCurry 2008). Over short timescales, inferences on the effects of mafic magma are generally focused around the associated influxes of heat and/or volatiles into the silicic system that may mobilize it and trigger eruptions (e.g. Sparks et al. 1977; Bachmann et al.

Always consult and cite the final, published document. See http:/www.minsocam.org or GeoscienceWorld

2002; Huber et al. 2011). As silicic magmatic systems act as density traps, evidence of the direct influence of mafic magmas on silicic systems is often limited to one or more of co-erupted mafic enclaves or mingled magmas, and up-temperature geochemical signals in the growth records of crystals in the eruption products (e.g. Sparks et al. 1977; Bacon and Metz 1984; Bachmann et al. 2002; Wilson et al. 2006; Pritchard et al. 2013; Barker et al. 2016; Singer et al. 2016; Stelten et al. 2017). The most primitive compositions are, however, often not represented in the co-erupted mafic components when compared with mafic magmas erupted away from the focus of silicic volcanism suggesting that some hybridization has taken place (e.g. Bacon and Metz 1984). Stalling of mafic magmas beneath a silicic system due to density trapping may serve to enhance the interaction of mafic magmas with host rocks and/or silicic magmas and the generation of distinct compositions not seen in adjacent areas (e.g. Wilson et al. 2006). Analysis of mafic inclusions, therefore, can give valuable insights into the thermal and chemical driving mechanisms beneath silicic systems. To illuminate these mechanisms, we here present data on the mafic compositions of inclusions and surficial lavas associated with the Yellowstone Plateau volcanic field, specifically those associated with the earliest caldera-forming cycle that generated the Huckleberry Ridge Tuff.

GEOLOGICAL SETTING

Yellowstone and the Snake River Plain

The Yellowstone Plateau volcanic field (YPVF) is the youngest (active since ~2.1 Ma) volcano-magmatic system at the northeastern end of the Yellowstone-Snake River Plain (YSRP) volcanic area (Christiansen 2001). The YSRP area is a 700 km long, NE-ward progressing volcanic province extending from eastern Oregon and northern Nevada to

Always consult and cite the final, published document. See http:/www.minsocam.org or GeoscienceWorld

northwestern Wyoming (Fig. 1; Pierce and Morgan 2009). The province contains a series of caldera complexes associated with voluminous silicic volcanism, followed by voluminous basaltic activity. The caldera systems were initiated at ~16 Ma in northernmost Nevada, broadly coincident with the eruption of the Columbia River Basalts to the north (e.g. Coble and Mahood 2012, 2015) and have migrated spasmodically eastward. Although the focus of silicic volcanism has migrated to the northeast (at a rate and in a direction corresponding to movement of the North American Plate over a fixed point), voluminous basaltic volcanism has persisted along the YSRP into Holocene time (Armstrong et al. 1975; Kuntz et al. 1992).

The northeastward propagating volcanism of the YSRP has been often been attributed to the movement of the North American plate over a stationary mantle plume, forming a 'hotspot track' (Pierce and Morgan 1992, 2009). This hypothesis is supported by the imaging of a weak thermal anomaly, inferred to represent material containing small degrees of partial melt, down to and across the 660 km discontinuity (Yuan and Dueker 2005; Smith et al. 2009; Schmandt et al. 2012). However, a high-velocity zone located in the mantle beneath the Snake River Plain and Yellowstone at ~400-500 km depth has been interpreted as a remnant of the subducted Farallon plate, that foundered beneath the western US at ~50 Ma (Schmandt and Humphreys 2011; James et al. 2011). The presence of this high-velocity zone has led to an alternative model for YSRP volcanism invoking poloidal asthenospheric upwelling around the foundering slab. It has been proposed that the northern and eastern edges of the slab serve to delineate the margins of the YSRP, creating a low-velocity zone observed in the upper mantle along the length of the YSRP (James et al. 2011; Zhou et al. 2017). This low-velocity zone is inferred to contain partial melt and to be hydrated, explaining the continuing basaltic volcanism along the SRP even after the termination of local silicic volcanism (Armstrong et al. 1975; Schmandt and Humphreys 2010;

DOI: https://doi.org/10.2138/am-2018-6273

James et al. 2011). However, despite the presence of the low-velocity zone along the length of the YSRP, elevated heat and mantle-derived-gas fluxes in the Yellowstone area (e.g. Hurwitz and Lowenstern 2014) require there to be a deep-seated thermal anomaly distinct from that extending westwards into the Snake River Plain.

Volcanism along the YSRP locus has typically been considered as bimodal. Olivine tholeiites dominate the mafic compositions and are inferred to provide heat to partially melt solidified, underplated tholeiitic intrusive forerunners which, in turn, become parental magmas to the voluminous ferroan rhyolites (Christiansen and McCurry 2008; McCurry and Rodgers 2009). Basaltic activity typically precedes and follows silicic volcanism at individual volcanic centers along the YSRP, with intervening periods of no basaltic volcanism while the silicic magmatic systems act as an effective density trap (Christiansen 2001). Petrological and isotopic studies collectively infer that the olivine tholeiites result from the hybridization of young, asthenosphere-derived melts with partial melts of the lithospheric mantle, which last equilibrated in an ancient, dry lithospheric mantle keel at depths of 70-100 km and at temperatures consistent with an only slightly elevated geothermal gradient (Doe et al. 1982; Hildreth et al. 1991; Hanan et al. 2008; Leeman et al. 2009). The basalts are also considered to show signatures of minimal crustal contamination on their rise to the surface (Doe et al. 1982; Menzies et al. 1984; Hildreth et al. 1991; Leeman et al. 2009). The tholeiites are dominantly olivine and plagioclase phyric with a notable lack of clinopyroxene, indicating minimal significant mid-crustal crystallization, where clinopyroxene would be the primary liquidus phase (Thompson 1975; Leeman et al. 2009). Olivine tholeiites erupted in the Yellowstone area are similar to those elsewhere in the Snake River Plain but extend to more evolved compositions (Christiansen and McCurry 2008). In addition to the olivine tholeiites, some mafic to minor silicic lavas of contrasting affinity are also found in the eastern Snake

Always consult and cite the final, published document. See http:/www.minsocam.org or GeoscienceWorld

River Plain. The mafic lavas, predominantly found at the Craters of the Moon lava field, form a distinctly alkalic trend characterized by high TiO_2, P_2O_5, Ba, Zr and rare-earth elements (REE), and lower MgO and CaO relative to olivine tholeiites and are referred to as the Craters of the Moon (COM) trend (Leeman et al. 1976; Christiansen and McCurry 2008; McCurry et al. 2008; Putirka et al. 2009).

Whether the silicic magma erupted in the YSRP province is generated through fractional crystallization (e.g. McCurry et al. 2008) or through partial melting of basaltic and/or felsic crust (e.g. Hildreth et al. 1991; Bindeman and Simakin 2014), a large amount of basaltic magma is required to provide heat, volatiles and fractionated material. The >3,700 km^3 of silicic magma erupted in the YPVF alone over the last ~2 Ma requires a voluminous supply of basaltic melt from the mantle to drive the silicic volcanism (Christiansen 2001; McCurry and Rodgers 2009; Stelten et al. 2017). This basaltic flux has also been inferred from the modern large thermal and He and CO_2 fluxes within the volcanic field (Hurwitz and Lowenstern 2014) and is linked to the imaging of a large (46,000 km^3) lower-crustal, melt-bearing body inferred to be basaltic in composition (Huang et al. 2015).

Although there is voluminous basaltic volcanism preceding and subsequent to the focus of silicic volcanism at Yellowstone, and its presence has been invoked as a key driver in the generation and triggering of rhyolitic bodies (e.g. Loewen and Bindeman 2015), there is a paucity of basaltic material erupted penecontemporaneously with the voluminous silicic eruptions (Christiansen 2001). Rarely in the volcanic field, and mostly in extra-caldera rhyolites, is evidence for magma mingling observed (Wilcox 1944; Pritchard et al. 2013). Therefore, previous inferences on the mantle inputs into Yellowstone have been solely derived from basalts erupted peripherally to the field or long after caldera formation (Doe et al. 1982; Hildreth et al. 1991; Hanan et al. 2008). To provide a contrasting perspective, we

Always consult and cite the final, published document. See http:/www.minsocam.org or GeoscienceWorld

here document the mafic components (including the 'scoria' previously described by Christiansen 2001) that were discharged during the large caldera-forming rhyolitic eruption of the Huckleberry Ridge Tuff. We compare their compositions to mafic (basaltic to andesitic) compositions erupted before and afterwards in the geographic area within and around the Huckleberry Ridge Tuff caldera to investigate the nature of the mafic lineages in this area and consider their likely origins.

The Huckleberry Ridge Tuff

The ~2.08 Ma, ~2,500 km^3 Huckleberry Ridge Tuff (HRT) is the product of the climactic eruption of the first of three volcanic cycles in the YPVF (Christiansen 2001; Rivera et al. 2014; Singer et al. 2014; Wotzlaw et al. 2015). The HRT consists of initial fall deposits, which are overlain by three ignimbrite packages (members A, B and C), with additional fall deposits beneath member C (Christiansen 2001).

The HRT eruption was shortly preceded by two episodes of volcanism, generating the rhyolitic Snake River Butte lava, and the lavas collectively mapped by Christiansen (2001) as the Junction Butte Basalt. Other precursory eruptions may well have occurred in areas now down-dropped and buried in the HRT and younger calderas, but any direct evidence for these is now lost. The Junction Butte Basalt is composed of multiple independent flows which crop out at the northern end of the Yellowstone Plateau and northeast of the mapped HRT caldera (Fig. 1; Christiansen 2001). Although the Junction Butte Basalt flows are amongst the least primitive mafic compositions erupted at Yellowstone (and Junction Butte itself is intermediate in composition), they are here grouped in with the SRP olivine tholeiites, albeit with these flows containing plagioclase phenocrysts and groundmass olivine (Hildreth et al. 1991; Christiansen 2001).

Always consult and cite the final, published document. See http:/www.minsocam.org or GeoscienceWorld

This is a preprint, the final version is subject to change, of the American Mineralogist (MSA)
Cite as Authors (Year) Title. American Mineralogist, in press.
DOI: https://doi.org/10.2138/am-2018-6273

SAMPLED MATERIALS

We present data here on eruptive materials from the Yellowstone area and for descriptive convenience group these into three suites (Table 1). These suites encompass juvenile mafic material erupted in the Huckleberry Ridge event, together with comparator lavas which are temporally close to the eruption and/or were erupted spatially adjacent to or within the HRT caldera. Sample and locality information are given in Supplementary Table 1.

Suite 1: HRT mafic materials. Although the HRT is composed dominantly of high-silica rhyolite, scoriaceous material has been reported as commonly present in the upper part of member B (Hildreth et al. 1991; Christiansen 2001). Reported analyses of this scoriaceous material (samples 81YH-79: Hildreth et al. 1984; 74IP-149B: Hildreth et al. 1991; Christiansen 2001), however, return rhyodacite compositions (70.5 and 70.8 wt % SiO_2 respectively). Extensive fieldwork on the HRT by Wilson shows, however, that there is a comparable juvenile mafic component in both ignimbrite members A and B (Table 1). This component matches physically the scoria described by Christiansen (2001) where it is found in upper ignimbrite B. However, our analyses yield greatly contrasting compositional characteristics when compared to the previously reported data. In member A, especially at exposures southwest of the caldera, poorly to non-vesicular clasts of dark-grey to greenish-grey, rarely red-oxidized material (Fig. 2a) occur within the dense-welded rheomorphic tuff attributed by Christiansen (2001) to member B, but identified by us as member A. Briefly, this identification is made on the basis that the relevant tuff can be traced continuously downwards to the HRT basal contact, and upwards to where a horizon representing a short

Always consult and cite the final, published document. See http:/www.minsocam.org or GeoscienceWorld

hiatus (reworked ash materials, minor welding reversal) separates the lower ignimbrite (i.e. A) from an upper ignimbrite unit that has scoria present in its upper parts (i.e. B). Non-vesicular mafic material is also rarely found in lower ignimbrite B in the same area southwest of the caldera. Moderately to highly vesicular black to purple- to red-oxidised scoria is also widespread as a component in mingled pumices (Fig. 2b) and as discrete lapilli-grade clasts in upper member B, as previously reported. We sampled individual clasts of the poorly vesicular material from ignimbrite A mostly from localities southwest of the caldera, and extracted the vesicular scoria from mingled pumices in upper ignimbrite B from a site southwest of the caldera where glassy, non-welded material occurs (Supplementary Table 1). Elsewhere, the discrete scoria clasts in upper ignimbrite B are either too small to sample effectively, or are vapor-phase altered and recrystallized along with their host tuff. Also, rare macroscopically mingled scoria clasts were found in member A and sampled, and are labelled as such here.

Suite 2: SRP olivine tholeiites. We sampled a selection of the lavas generally attributed to the SRP olivine tholeiite suite (Supplementary Table 1), including several examples reported on by Hildreth et al. (1991). These lavas represent flows (i) pre-dating the HRT and exposed around the caldera margin (including one example underlying the HRT southwest of the caldera), and (ii) post-dating the HRT, forming part of the extensive flows flooring the Island Park segment of the combined HRT and Mesa Falls Tuff-related calderas, and elsewhere in the Yellowstone caldera.

Suite 3: COM eruptives. We sampled pyroclasts from several scoria cones linked to young eruptions of the COM suite in the Spencer-High Point Field (Fig. 1; Supplementary Table 1). These cones were sampled from an area on, or immediately west of, the western

Always consult and cite the final, published document. See http:/www.minsocam.org or GeoscienceWorld

rim of the mapped HRT caldera and were selected on the basis of information in Iwahashi (2010).

Published data. We compare our data from all three suites to published data from spatially and chemically comparable deposits. The Suite 2 literature field comprises data from olivine tholeiites along the Yellowstone-Snake River Plain volcanic area (but does not include data from the Columbia River Basalt group). This field also includes examples of olivine tholeiites from the Craters of the Moon lava field (NEOT flows of Putirka et al. 2009), from the Spencer-High Point Field (Type 1 flows of Iwahashi 2010) and compositions from two databases: the North American Volcanic Rock Data Base (NAVDAT: http://www.navdat.org/) and the Geochemistry of Rocks of the Oceans and Continents (GEOROC: http://georoc.mpch-mainz.gwdg.de/georoc/). Published data for Suite 3 comparisons were derived from studies of the Craters of the Moon area (Leeman 1974; Leeman et al. 1976: COME flows of Putirka et al. 2009) and from the Spencer-High Point Field (Type 2 flows of Iwahashi 2010). All mafic data (i.e. <65 wt% SiO_2, the range of compositions analyzed in this study) were selected based on location, as we did not want to restrict comparisons to basalts only (cf. Hildreth et al. 1991). No screening for perceived contamination or primitive compositions was undertaken so as to allow us to compare compositional ranges and degrees of evolution in all suites related to the broad range of petrogenetic processes occurring in volcanic rocks in this region.

ANALYTICAL METHODS

Samples from the three suites were collected and any adhering matrix or visible xenocrysts removed by hand picking to isolate the mafic component. In two clasts (YP185

Always consult and cite the final, published document. See http:/www.minsocam.org or GeoscienceWorld

and YP188, both from early member A) mingling was too complex to allow complete separation. These clasts therefore represent a mixture of mafic and rhyolitic components (denoted by 'M' in geochemical plots). Samples were subsequently crushed and milled in an agate Tema mill to yield a homogenous powder. Powders were analyzed for major element concentrations by X-ray fluorescence (XRF) at the Open University (OU), UK and at the University of Auckland, New Zealand following the methods of Ramsey et al. (1995). Replicate analyses of standards give approximate 2 standard deviation (2sd) external precisions of <3% for all elements, with most <1% (Electronic Appendix 1). Accuracies are within 5% for all elements compared to preferred values for replicate standard analyses. Duplicates run between institutions show <5% offset for all elements with >0.1 wt% abundance. Trace element concentrations were measured by solution inductively-coupled plasma mass-spectrometry (ICP-MS) at the OU and Victoria University of Wellington, New Zealand (VUW) using an Agilent 7500 and a Thermo Scientific Element2 sector-field ICP-MS, respectively. Abundances of trace elements were calculated by external normalization relative to a bracketing standard (BHVO-2). A secondary standard (BCR-2) was used to estimate external precisions, which were <6-7% for most elements except Li, Nb, Cs, Lu, Ta, Tl, Pb, Th, U, Ni Cu, Zn (<20%) and Mo (>20%). Accuracies are <6-7% for all elements, apart from Ta, Tl, Cu (<15%) and Mo (>15%).

Isotope analyses were conducted using a Finnigan Triton Thermal Ionization Mass-Spectrometer (TIMS) in the laboratories at the OU and VUW, but on the same instrument. Chromatographic element separation was based on the procedure of Pin et al. (2014; see Supplementary Material for more information). Sr was analyzed on single Re filaments, using a TaF_2 activator (Charlier et al. 2006), for 240 ratios with an integration time for each ratio of 16.777 s. Measurements were internally normalized to $^{86}Sr/^{88}Sr = 0.1194$ and Rb

Always consult and cite the final, published document. See http:/www.minsocam.org or GeoscienceWorld

interference was corrected by measuring ^{85}Rb and applying a correction using ^{87}Rb/^{85}Rb = 0.385707 (Rosman and Taylor 1998). Repeated analyses of NBS987 yield an average of 0.710254 ± 0.000015 (2sd, n=16). Isotopic ratios from different runs were normalized to a value of 0.71025 for NBS987, the long-term mean reported by Thirlwall (1991). Procedural blank was 110 pg, insignificant when compared to the ~ 1000 ng loaded onto each filament and thus necessitated no blank correction.

Nd was analyzed on double Re filaments with a H_3PO_4 loading solution over 270 ratios with an integration time of 8.389 s for each measurement. Ratios were internally normalized using a value of ^{146}Nd/^{144}Nd = 0.7219 and any presence of Ce and Sm corrected using values of ^{140}Ce/^{142}Ce = 7.97297 and ^{144}Sm/^{147}Sm = 0.20667 (Rosman and Taylor 1998). Repeated analyses of standards J&M (internal) and La Jolla yield values of 0.511818 ± 0.000004 (2sd, n=11) and 0.511845 ± 0.000002 (2sd, n=3) respectively, the former consistent with the long-term laboratory average (0.511821 ± 0.000002 2sd) and the latter similar to 0.511856 ± 0.000007 (2sd) measured by Thirlwall (1991). Procedural blank was 8 pg and thus warranted no blank correction.

Pb was analyzed using a double-spike method (see Todt et al. 1996). Half the sample (approximately 150 ng), was run naturally on single Re filaments for 180 ratios using a silica gel activator (Gerstenberger and Haase 1996). Subsequently, the remaining sample and a ^{207}Pb/^{204}Pb double spike (Thirlwall et al. 2000) was thoroughly admixed mixed and analyzed on single Re filaments for 120 ratios in the same way as the natural run. Integration times for both runs were 8.389 s. The data were then deconvolved to determine the isotopic ratios. Values for NBS981 were ^{206}Pb/^{204}Pb = 16.945 ± 0.001, ^{207}Pb/^{204}Pb = 15.503 ± 0.001 and ^{208}Pb/^{204}Pb = 36.737 ± 0.004 (2sd, n = 32). Isotopic measurements from different runs

Always consult and cite the final, published document. See http:/www.minsocam.org or GeoscienceWorld

were normalized to the values of Todt et al. (1996). The procedural blank for Pb was 10 pg and warranted no correction.

RESULTS

Full major element, trace element and isotopic data for the samples analyzed in this study are given in Electronic Appendix 1, and a representative selection of analyses is given in Tables 2 and 3.

Major elements

HRT mafic dense and scoria clasts (hereafter HRT mafics, constituting Suite 1) form a coherent trend from 49-63 wt% SiO_2, regardless of their stratigraphic position or degree of vesiculation. They are characterized by high alkalis (Na_2O + K_2O = 4.5-7.3 wt%: Fig. 3a), P_2O_5 (0.52-1.8 wt%; Fig. 3b), TiO_2 (1.5-3.5 wt%) and FeO (9.6-16.1 wt%; Supplementary Fig. 1). Suite 1 samples also have low MgO (0.6-3.0 wt%) and CaO (1.6-7.2 wt%; Supplementary Fig. 1) values.

Samples from flows with olivine tholeiitic affinity (Suite 2) erupted throughout the volcanic history of Yellowstone form a coherent compositional group with SiO_2 ranging from 46-54 wt%. They are distinct from Suite 1 samples with higher MgO (4.2-11 wt%) and CaO (7.7-11 wt%; Supp. Fig. 1), which are negatively correlated with SiO_2, and contain low total alkalis (Na_2O+K_2O; 2.4-4.7 wt%; Fig. 3a) and P_2O_5 (0.19-0.62 wt%; Fig 3b). Mg# values (defined as Mg# = $100[X_{MgO}/(X_{MgO}+X_{FeO})]$ where FeO = $0.9[Fe_2O_3$ (T)] on a wt% basis) of up to 64 show that the primitive end of the range in YSRP tholeiites is represented in our Yellowstone Suite 2 samples (cf. Leeman et al. 2009).

Always consult and cite the final, published document. See http:/www.minsocam.org or GeoscienceWorld

There are broad major element similarities between our COM-type samples (Suite 3) and HRT mafics (Suite 1). Suite 3 samples cover a similar SiO_2 range to Suite 1 samples (47-57 wt%), with similarly high FeO (10-14 wt%), TiO_2 (up to 3.0 wt%; Supplementary Fig. 1) and P_2O_5 (0.60-2.2 wt %; Fig. 3b), and depletions in MgO (1.6-3.7 wt%) and CaO (4.7-8.3 wt%) when compared to the olivine tholeiites. Their compositions are mildly alkalic (total alkalis 5.0-7.6 wt%; Fig. 3a) and are similar to the published COM-trend for rocks with this silica percentage (Fig. 3; Leeman et al. 1976; Christiansen and McCurry 2008; Putirka et al. 2009). Note, however, that in general, the Suite 1 HRT mafic compositions form arrays in Harker plots that are parallel to, but slightly offset from, our Suite 3 samples and the overall COM fields (see Fig. 3), particularly with respect to lower total alkalis, P_2O_5, and TiO_2 in the Suite 1 samples.

Trace elements

The clear separation between the Suite 1 HRT mafic samples and Suite 3 COM-type samples when compared to the Suite 2 olivine tholeiites is also apparent in trace element abundances. The Suite 1 HRT mafics and Suite 3 COM-type materials have notably high concentrations of incompatible elements including large-ion lithophile elements (LILE), e.g. Rb (25-99 ppm; Supplementary Fig. 2a) and Ba (1120-3800 ppm: Fig. 4a), high field strength elements (HFSE), e.g. Zr (660-1970 ppm: Fig. 4b) and Nb (29-87 ppm), and actinides e.g. U (1.2-3.5 ppm with outliers at 4.7 and 5.7 ppm). In contrast, olivine tholeiite samples have notably higher V (210-280 ppm; Supplementary Fig. 2c), Ni (26-190 ppm) and Cr (20-540 ppm). Sr concentrations are similar among both the mafic suites 1 and 3 (140-550 ppm; Supplementary Fig. 2b) and within the range defined by our Suite 2 olivine tholeiite samples. Suite 1 HRT mafic and Suite 3 COM-type samples are elevated in all rare-earth elements

Always consult and cite the final, published document. See http:/www.minsocam.org or GeoscienceWorld

(REE) relative to the Suite 2 olivine tholeiites and have sub-parallel trends (Fig. 5) with $(La/Yb)_N$ ratios (5.0-10 with outlier YP242 at 18) overlapping with those of the olivine tholeiites (2.6-11). Zr/Hf ratios are elevated in the Suite 1 (47-61) and Suite 2 samples (52-55) relative to the Suite 3 samples (40-49) but other incompatible element ratios are similar between the different suites (e.g. Ce/Pb: Supplementary Fig. 3).

The only major divergence between the trace element compositions of the Suite 1 HRT mafic samples and Suite 3 COM-samples is in Ba where there are two apparent trends when plotted versus SiO_2 (Fig. 4a). The moderate Ba trend in our Suite 3 samples aligns with the typical COM-trend reported elsewhere (Leeman et al. 1976; Christiansen and McCurry 2008) whereas the Suite 1 HRT mafic samples define a parallel trend with roughly double the Ba concentrations at a given value of SiO_2 (Fig. 4a).

Isotopic ratios

$^{87}Sr/^{86}Sr$ values for all samples range from 0.70373-0.70808, with the highest and lowest values measured from Suite 2 olivine tholeiite samples, similar to the range of 0.70377-0.70886 reported by Hildreth et al. (1991) from Yellowstone basalts. Suite 3 samples are tightly clustered (0.70574-0.70585) with one outlier (YR425: 0.70788 ± 0.00004 2se; Fig. 6). Suite 1 HRT dense mafics and scoria have broadly similar $^{87}Sr/^{86}Sr$ values (0.70709-0.70771), which are more radiogenic than our Suite 3 COM-type samples (Fig. 6, 7). However, both suites are notably less radiogenic than the COM samples reported on by Putirka et al. (2009: $^{87}Sr/^{86}Sr$ = 0.70784-0.71130) and Leeman (1974: $^{87}Sr/^{86}Sr$ = 0.70810-0.71240). $^{87}Sr/^{86}Sr$ variations in the Suite 1 HRT mafic samples correlate positively with respect to whole-rock Rb/Sr ratios (R^2 = 0.65) whereas the olivine tholeiites show isotopic

Always consult and cite the final, published document. See http:/www.minsocam.org or GeoscienceWorld

variability at similar Rb/Sr ratios (Fig. 7a). There is no clear correlation between $^{87}Sr/^{86}Sr$ and 1/Sr in any of our samples (Fig. 7b).

In similar fashion to Sr, the full range in $^{143}Nd/^{144}Nd$ values (0.51207-0.51251) for our data is spanned by Suite 2 olivine tholeiite samples (Fig. 6). HRT dense mafic clasts from ignimbrite A (0.51218-0.51232), HRT vesicular scoria from ignimbrite B (0.51231-0.51235) and Suite 3 samples (0.51225-0.51240) all cover similar, largely overlapping ranges. All samples give negative ε_{Nd} values (-2 to -10), where

$$\varepsilon_{Nd} = \left[\frac{\left({}^{143}Nd/{}^{144}Nd\right)_{meas}}{\left({}^{143}Nd/{}^{144}Nd\right)_{CHUR}} - 1\right] \times 10^4$$

from DePaolo and Wasserburg (1976). A value of CHUR (chondritic uniform reservoir) of 0.51263 was used, from Bouvier et al. (2008). Three of four Suite 3 samples have Nd isotopic values very similar to the median of Yellowstone-Snake River Plain basalts (0.512405: McCurry and Rodgers 2009), whereas three of four Suite 2 samples have ratios more radiogenic than the median and the Suite 1 samples are less radiogenic. However, all except three samples (one from each suite), have ε_{Nd} values >-7, below which value basalts are interpreted by McCurry and Rodgers (2009) to be contaminated. There is also no clear correlation in any of the suites between $^{143}Nd/^{144}Nd$ and $^{87}Sr/^{86}Sr$ (Fig. 6).

Pb isotopic compositions also follow Sr and Nd in showing the greatest range in the Suite 2 olivine tholeiite samples ($^{206}Pb/^{204}Pb$ = 15.86-17.64; $^{207}Pb/^{204}Pb$ = 15.27-15.53; $^{208}Pb/^{204}Pb$ = 36.47-38.23: Fig. 8). In contrast in Suite 1, HRT dense mafics ($^{206}Pb/^{204}Pb$ = 16.88-16.95; $^{207}Pb/^{204}Pb$ = 15.45-15.46; $^{208}Pb/^{204}Pb$ = 37.92-37.94) and HRT vesicular scoria ($^{206}Pb/^{204}Pb$ = 16.95-16.98; $^{207}Pb/^{204}Pb$ = 15.48; $^{208}Pb/^{204}Pb$ = 38.02-38.03) show much more restricted ranges with the scoria being more radiogenic. Our Suite 3 COM-type samples ($^{206}Pb/^{204}Pb$ = 17.16-17.36; $^{207}Pb/^{204}Pb$ = 15.48-15.51; $^{208}Pb/^{204}Pb$ = 38.07-38.15) also show a

Always consult and cite the final, published document. See http:/www.minsocam.org or GeoscienceWorld

modest range. Suite 1 samples collectively form a sub-parallel trend to the Suite 2 olivine tholeiite samples, offset to higher $^{207}Pb/^{204}Pb$ for a given value of $^{206}Pb/^{204}Pb$ (Fig. 8). All except one sample (the $^{207}Pb/^{204}Pb$ composition of Basalt of the Narrows [YR292], which also has notably unradiogenic Sr isotopic characteristics) plot above the Northern Hemisphere Reference Line (Hart 1984).

DISCUSSION

The context of the HRT mafic magmas

In considering the nature and range of compositions of the Suite 1 HRT mafic compositions and the comparator materials from suites 2 and 3 there are two aspects that need to be borne in mind. First, as seen elsewhere (e.g. Bacon and Metz 1984; Hildreth et al. 1991; Wilson et al. 2006; Pritchard et al. 2013), these mafic compositions related to silicic systems show features in their trace element and isotopic characteristics that suggest they do not generally represent pristine melts or magmas coming directly from a uniform mantle source. Even the least evolved compositions sampled in each of the case studies cited above show evidence for some variability in the mantle source, and/or fractionation or assimilation, but when and where these processes occurred is open to debate, as is the role of mantle versus crustal processes (cf. Rasoazanamparany et al. 2015). Second, the mafic compositions sampled in single silicic eruptions are rarely uniform in composition (see examples cited above), and the processes whereby the compositional variations within each suite are generated also need to be considered.

In addition, there needs to be taken into consideration the regional setting of the HRT mafics we document. Although lavas of olivine tholeiite affinity were erupted before

Always consult and cite the final, published document. See http:/www.minsocam.org or GeoscienceWorld

and after the HRT in the Yellowstone area, major and trace element characteristics of the Suite 1 HRT mafics show closer links with COM-type compositions represented here by Suite 3 samples from the late Pleistocene Spencer-High Point volcanic field. The latter eruptives have been in turn been linked with distinctly alkalic lava flows from the Craters of the Moon lava field (Kuntz et al. 1992; Iwahashi 2010). The Craters of the Moon lava field consists of ~30 km^3 of late Quaternary (~15-2.1 ka) lava flows, erupted from monogenetic and polygenetic vents along a volcanic rift zone, the 85 km long Great Rift in the eastern Snake River Plain (Fig. 1: Kuntz et al. 1986). During the total lifespan of the Craters of the Moon lava field, several other olivine tholeiite lava fields were erupted in the eastern Snake River Plain, two of which (Kings Bowl and Wapi lava fields) were also sourced from the Great Rift (Fig. 1) and were contemporaneous with the final eruptive phase of the Craters of the Moon lava field (Kuntz et al. 1986, 1992).

The contemporaneity of young COM and olivine tholeiitic lavas along the Great Rift is analogous to what we report here from the HRT, which occurred between episodes of olivine tholeiite extrusion. This complexity within the YPVF has not been recognized before, with the prevailing view being that olivine tholeiites dominate the YPVF mafic suite and are intimately linked to the rhyolites (e.g. Hildreth et al. 1991; Christiansen and McCurry 2008). It is thus apparent that the sharp contrasts in composition between the COM and olivine tholeiite magma types reflect sources and processes that can act contemporaneously to feed vents contained within quite limited geographic areas.

In the subsequent discussion, we first consider the various controls on the compositions of the least-evolved magmas erupted within the three suites reported on here, and in particular address whether the Suite 1 HRT mafics could be generated from the same source region/primary magma as gave rise to the volumetrically dominant olivine tholeiites

Always consult and cite the final, published document. See http:/www.minsocam.org or GeoscienceWorld

at Yellowstone and elsewhere in the SRP. Evidence for and against each of the processes put forward is summarized in Table 4. We then focus on the variability within each of the suites in order to address whether these variations follow a common pattern, or whether there are unique features to the compositional variations shown within each suite. Finally, we compare and contrast our data and inferences with the published array of compositional information on SRP volcanism, with particular reference to the main Craters of the Moon area.

Generation of the parental magma for the Suite 1 HRT mafic compositions

The least evolved of the Suite 1 HRT mafics (Table 2) has a bulk SiO_2 composition close to those of the olivine tholeiites in the Yellowstone area (Suite 2 data, and Hildreth et al. 1991), but radically contrasting values for many major and trace elements (Table 2, Figs. 3, 4). We here consider the diverse and sometimes contradictory models (summarized in Table 4) proposed for generation of the parental COM-type magmas (including our Suite 3 samples) and compare them against the data we present here for the Suite 1 HRT mafics.

Fractional crystallization. The most commonly invoked mechanism for generation of magmas in the COM-trend in general has been through extreme fractional crystallization of an olivine tholeiite parent (Christiansen and McCurry 2008; McCurry et al. 2008). In support of this view, experimental studies by Whitaker et al. (2008) derived liquids with major element compositions similar to primitive COM lava flows through ∼80 % crystallization (∼40 % plagioclase, ∼22 % olivine and ∼18 % pyroxene) of an olivine tholeiite starting material at 1,100 °C, 4.3 kbar and 0.4 wt% H_2O. However, there was also early recognition that fractional crystallization alone cannot completely replicate the observed compositional variations, particularly with regard to trace elements (Leeman et al. 1976). Our Suite 1 HRT

Always consult and cite the final, published document. See http:/www.minsocam.org or GeoscienceWorld

mafics data allow us to consider a fractional crystallization mechanism through simple modeling of trace elements to try and replicate the distinctive signatures of the least evolved members of the suite. Fractional crystallization modeling used the Rayleigh fractionation equation:

$$\frac{C_L}{C_O} = F^{(\overline{D}-1)},$$

where C_L and C_O are the elemental concentrations in the derived and original liquids respectively, F is the fraction of melt remaining and $\overline{D}$ is the bulk distribution coefficient:

$$\overline{D_a} = \sum W_B D_{aB},$$

where W_B is the weight % of the mineral B in the rock and D_{aB} is the distribution coefficient of element a in mineral B.

Warm River basalt (sample YR291) was used as the starting composition due to its similarity in composition to the starting material of Whitaker et al. (2008) and it having characteristics of a relatively 'primitive' lava (e.g. Mg# of 64.1 [Leeman et al. 2009] with high Ni and Cr: Table 2). Using $\overline{D}$ = 0 (i.e. perfect incompatibility) for Ba, Zr, Rb, U, Hf, Th, and Y, ≥84% crystallization generates liquids similar in major element composition to the aphyric samples at the least-evolved end of our HRT Suite 1 samples. This degree of crystallization is similar to that proposed by Whitaker et al. (2008) from experimental studies. To test this possible fractionation pathway, we model Sr values on the basis that the experimental and petrographic crystal assemblages are dominated by plagioclase in which Sr is compatible. To generate a composition similar to the HRT suite with ~84% crystallization, $\overline{D}$ = 0.7 is required. Using the partitioning relationship of Sr in plagioclase from Blundy and Wood (1991), at a temperature of 1,100 °C (Whitaker et al. 2008; Putirka et al. 2009) and X_{An} = 0.63 (Whitaker et al. 2008), D_{Sr} = 2.4, (similar to D_{Sr} = 2.31 at 1194 °C, 5 kbar and An = 0.59

Always consult and cite the final, published document. See http:/www.minsocam.org or GeoscienceWorld

proposed by Sun et al. 2017). Based on the experimental crystallization of 50% plagioclase, and ignoring the minimal effects of olivine and clinopyroxene on the Sr partition coefficient, this approach would yield a value of $\overline{D}_{Sr}$ = 1.4 and generate Sr-depleted melts (105 ppm with 84% crystallization) that have lower Sr concentrations than any Suite 1 samples analyzed in this study (Electronic Appendix 1; Fig. 9). Using only the most calcic plagioclase composition (X_{An} = 0.85) from Putirka et al. (2009), with the other parameters unchanged, would a plagioclase D_{Sr} = 1.4 and therefore a required $\overline{D}_{Sr}$ = 0.7 be generated. Although it is possible to replicate the observed patterns with variable Sr partition coefficients, we additionally note that there are no strong negative Eu anomalies in any Suite 1 samples (Fig. 5), which would be expected with significant plagioclase fractionation. A similar degree of fractionation (>80%) would be required to generate the Eu signature of the HRT Suite 1 samples with D = 0, a very unlikely situation in a plagioclase-dominated assemblage. Using D_{Eu} = 2.39 at 1194 °C, 5 kbar and An = 0.59 (Sun et al. 2017), a resulting $\overline{D}_{Eu}$ = 1.2 would generate melts depleted in Eu (0.6 ppm with 84% crystallization), the opposite to what is seen (Fig. 5). Therefore we consider extreme fractionation of an olivine tholeiite parent to be not viable as the sole or even necessarily a major mechanism for the generation of the parental Suite 1 HRT compositions.

Crustal assimilation. Another possibility to generate the least-evolved HRT Suite 1 melts is assimilation of crustal rocks by olivine tholeiites as they ascend. Any variations within the HRT suite, e.g. Ba (Fig. 4a), would then be explained through varying degrees of assimilation. In this context, Geist et al. (2002) proposed assimilation of a P-rich ferrogabbro, whereas Putirka et al. (2009) proposed a two-stage assimilation-fractional crystallization (AFC) model. The latter invoked early assimilation of 'mafic pods' in the lower crust followed by mid-crustal assimilation of wall-rocks similar in composition to the rhyolite inclusions

Always consult and cite the final, published document. See http:/www.minsocam.org or GeoscienceWorld

reported from the COM suite (but not found in the centers sampled for this work). We use a similar approach to Putirka et al. (2009) here to evaluate possible assimilants to explain the least evolved Suite 1 HRT mafic compositions.

To generate the HRT primitive end-member through dominantly assimilation processes requires that the assimilant has elemental concentrations at least as high as that end-member. NAVDAT and GEOROC databases were thus used to search for plausible end members (see Electronic Appendix 2 for search parameters). Although no results fitted the search criteria in NAVDAT, 18 samples were returned from GEOROC, predominantly lamproites. Although these samples have the low-moderate SiO_2 (37-59 wt%) required to be a plausible assimilant, they are generally much higher in Sr, with all except one with Sr concentrations least twice as high (>1110 ppm), and with K_2O values mostly greater than three times the concentration of any Suite 1 sample at a given SiO_2 concentration. Furthermore, the REE trend of the GEOROC sample group is very unlike the sub-parallel trends of the olivine tholeiites and HRT suites, being highly LREE enriched and having $(La/Yb)_N$ ratios (≥52) at least three times those of any samples reported here. Any AFC trend with a lamproitic or similar assimilant would then require a second AFC stage with a strongly heavy-REE enriched assimilant of which a composition has yet to be found. Additionally, although lamprophyres occur on the Colorado Plateau and in Wyoming, they have low Zr and high Sr concentrations (Mirnejad and Bell 2006; Lake and Farmer 2015), contrasting strongly with the Suite 1 mafics.

Considering other possible assimilants, rhyolite and granulite xenoliths found in lavas along the SRP have low TiO_2, lower REE abundances and, in most cases, steeper REE slopes than their host lavas (Leeman et al. 1985), antithetic to the elevated TiO_2, parallel REE trends but enriched concentrations of the least-evolved Suite 1 melts compared to Suite 2

Always consult and cite the final, published document. See http:/www.minsocam.org or GeoscienceWorld

parental compositions. Another characteristic precluding a strong control of assimilation on magma genesis is the high FeO of the Suite 1 parental compositions. The GEOROC comparator samples, with the exception of one, and COM rhyolite inclusions have lower FeO contents than olivine tholeiites (<7.4 and <3.5 wt% respectively) and thus cannot cause the FeO increase required to generate the Suite 1 parent from an olivine tholeiite. Furthermore, the lower K/Ba, and similar K/Rb with increasing SiO_2 in the Suite 1 samples relative to Suite 2 samples (Supplementary Fig. 4), which ratios would be expected to increase and decrease, respectively, with crustal assimilation, argue against significant contamination (as concluded by Leeman et al. 1976). High K/Ba values occur in HRT rhyolitic samples (Hildreth et al. 1991), assimilation of which would lead to increased K/Ba in the basalts, as is observed particularly in Suite 2 samples. Nevertheless, these HRT analyses have <650 ppm Zr, values that would be insufficient to generate the Suite 1 mafic parent through assimilation alone. There is an apparent trend defined by scoria samples (Fig. 4) with a visibly mingled sample (YP188) at the silicic end. However, this trend is antithetic to that of the overall Suite 1 mafics, indicating that mixing with rhyolite is not a plausible general mechanism for generation of the overall Suite 1 geochemical characteristics. Furthermore, the HRT rhyolites have Zr/Nb ratios of 4-13 (Hildreth et al. 1991). Mixing with rhyolite would require a mafic end-member Zr/Nb ratio of >50, which in turn would require the presence of an implausible and unseen Nb-rich phase (Fig. 9).

All samples analyzed in this study have higher Sr and lower Nd isotopic signatures than normal mantle-derived magmas, but which are consistent with values in basalts from the Yellowstone-Snake River Plain area that have equilibrated with lithospheric mantle (Fig. 6; Hanan et al. 2008; McCurry and Rodgers 2009). The elevated $^{87}Sr/^{86}Sr$ ratios of the published COM-type compositions relative to olivine tholeiites have been used to suggest

Always consult and cite the final, published document. See http:/www.minsocam.org or GeoscienceWorld

that crustal contamination is important in the generation of the COM-type parent (Leeman and Manton 1971; Menzies et al. 1984; Putirka et al. 2009). In contrast, the Suite 1 HRT mafic $^{87}Sr/^{86}Sr$ values are bracketed by our olivine tholeiite data, and all suite 1 and 3 samples fall within the broad field of SRP basalts (Fig. 6). It is possible that Suite 2 olivine tholeiites may have assimilated small amounts of very radiogenic Archean upper crust, whereas suites 1 and 3 magmas assimilated larger amounts of moderately radiogenic lower crust. From the perceived off- and on-axis spatial relationships of the COM-type and olivine tholeiites respectively, it has been argued that the ascent of the former is hindered by passage through primary granitic crust compared to the relatively fast ascent of the olivine tholeiites through crust replaced by basaltic sills (Christiansen and McCurry 2008; Putirka et al. 2009). A similar explanation for the differences between the least evolved samples from suites 1 and 2 presented here is difficult to uphold. This difficulty arises from the close spatial and temporal proximity of the earliest olivine tholeiite eruptions, the Junction Butte Basalt, traditionally viewed as contaminated, ($^{87}Sr/^{86}Sr = 0.70562 \pm 0.00004$ and 0.70756 ± 0.00004 2se, in our examples), to the HRT mafics ($^{87}Sr/^{86}Sr$ = 0.70709-0.70771). All these compositions were erupted at the beginning of known Yellowstone volcanism when the least replacement of the pre-existing crust would be expected to have occurred.

Depth/degree of partial melting. Another possible mechanism for generating mafic melts with differing chemical characteristics in the same geographic area is through source partial melting variations. Leeman et al. (2009) proposed that the Snake River Plain olivine tholeiites reflected melting of and equilibration with a spinel lherzolite source containing minimal or no garnet at 70-100 km depth (≤ 2.8 GPa). They cited the flat chondrite-normalized REE trends of primitive Snake River Plain olivine tholeiites, and low chondrite-normalized Gd/Yb ratios ($[Gd/Yb]_N$ = 1.1-1.7) which would increase strongly if there was

Always consult and cite the final, published document. See http:/www.minsocam.org or GeoscienceWorld

residual garnet in the source. The parallel REE slopes of the suites 1 and 3 samples when compared to those of Suite 2 (Fig. 5) suggest, however, that there was no significant difference in the depth of melting, consistent with the overlapping $(Gd/Yb)_N$ values of samples from Suite 2 (1.4-2.5) versus suites 1 and 3 (1.5-2.8).

Isotopic ratios of the different mafic suites can also provide clues on their source zones. The slope of the Suite 2 olivine tholeiite $^{207}Pb/^{204}Pb$ and $^{206}Pb/^{204}Pb$ ratios (Fig. 8), if interpreted as a pseudochron, gives an age of 2.77 ± 0.52 Ga (Supplementary Fig. 5a). This apparent age is broadly comparable to the 'secondary-isochron' age of 2.5 Ga reported by Doe et al. (1982), and a 2.8 Ga age from crustal xenoliths, the latter inferred to represent establishment of the Wyoming craton (Leeman et al. 1985). Similar pseudochrons can be regressed through data from our Suite 1 mafic samples (3.0 ± 0.22 Ga; excluding YP122; Supplementary Fig. 5b) and Suite 3 samples (2.56 ± 1.1 Ga; Supplementary Fig. 5c). The similar pseudochron ages between all three mafic suites indicate, based on our earlier conclusion that assimilation has been minimal, that the melts of all three mafic suites equilibrated with similar Archean-age regions. This inference, coupled with the unradiogenic and overlapping $^{143}Nd/^{144}Nd$ isotope ratios between the different mafic suites (Fig. 6) and, with the exception of one sample from our data set, plotting above the Northern Hemisphere Reference Line (Fig. 8), collectively require sources for all three suites within regions with ancient U and Nd enrichment. As the Suite 2 olivine tholeiite values are taken to indicate that they last equilibrated with Archean subcontinental lithospheric mantle (Doe et al. 1982; Hanan et al. 2008; Leeman et al. 2009), then the similarity in REE patterns and Pb and Nd isotopic systematics requires that our suites 1 and 3 compositions also last equilibrated with a similar source with a similar Archean history.

Always consult and cite the final, published document. See http:/www.minsocam.org or GeoscienceWorld

We now consider the possibility of varying degrees of partial melting of this common source to generate the contrasts between the different suites, using Ba, Nb and Zr as discriminants. Although all three elements are incompatible with respect to mantle mineral assemblages, their degrees of incompatibility vary, with Ba > Nb > Zr (D_{Ba} = 0.01, D_{Nb} = 0.04, D_{Zr} = 0.08: Hofmann 1988). Therefore, smaller degrees of partial melting than that associated with the olivine tholeiites should lead to elevated Ba/Nb, Ba/Zr and Nb/Zr ratios in the resulting melts. Although the Suite 1 mafics show elevated Ba/Nb ratios, their Nb/Zr ratios are lower and negatively correlated with Ba/Nb (this is also seen in Suite 3 samples). These relationships are the opposite to what would be expected were the Suite 1 mafics were derived from smaller-degree partial melts from a source common to the olivine tholeiites (Supplementary Fig. 6). Our data are thus consistent with variations within the olivine tholeiites being due to varying degrees of partial melting (Leeman et al. 2009) but extrapolation of this hypothesis to generation of the parental melts for suites 1 and 3 is incompatible with our data.

Enrichment of the mantle source. We next consider the possibility that magmas of suites 1 and 3 were generated from mantle sources contrasting in some respect to the Suite 2 samples. Although the ferroan and isotopically more crustal nature of the least evolved COM lavas have led to this possibility being dismissed by earlier workers (e.g. Leeman and Manton 1971; Leeman et al. 1976; Reid 1995; Putirka et al. 2009), Suite 1 compositions show contrasts with these 'type' COM flows (see subsequent section) that make a mantle contrast worth investigating. Differing mafic compositions erupted within a single volcanic field or province have elsewhere been attributed to source heterogeneity, with origins in regions of variably enriched or metasomatized mantle (e.g. Feeley 2003; McGee et al. 2013; Rasoazanamparany et al. 2015). Aqueous fluid has often been invoked as a mechanism for

Always consult and cite the final, published document. See http:/www.minsocam.org or GeoscienceWorld

DOI: https://doi.org/10.2138/am-2018-6273

locally enriching mantle sources, particularly in subduction zones through dehydration of the subducting slab (e.g. McCulloch and Gamble 1991). Such aqueous-rich fluids are typically enriched in LILE, and depleted in HFSE and REE that remain in the slab (McCulloch and Gamble 1991; Green and Adam 2003, and references therein).

Eocene subduction and source enrichments associated with the Farallon slab have previously been invoked in the timing and characteristics of the 55-45 Ma Absaroka Volcanic Province, overlapping with the eastern border of Yellowstone (Fig. 1: Christiansen and Yeats 1992; Feeley 2003; Schmandt and Humphreys 2011). The calc-alkaline, andesitic Absaroka eruptives have eastward-increasing K_2O contents and elevated LILE/HFSE ratios (Fig. 10: Chadwick 1970; Feeley 2003). These features have been linked to partial melting of a lithospheric mantle source that had been metasomatically enriched at <100 Ma by aqueous fluids derived from the Farallon slab (Feeley 2003). As the slab foundered, asthenospheric upwelling is proposed to have led to partial melting of the enriched region and generation of Absaroka magmas. A comparable scenario has also been invoked for other volcanic fields in the western U.S. (e.g. Mirnejad and Bell 2006; Lake and Farmer 2015; Brueseke et al. 2018). A modern low-velocity layer atop the mantle transition zone beneath the YSRP has also been attributed to a zone of partial melt caused by ascending volatiles from a still-dehydrating Farallon slab (Hier-Majumder and Tauzin 2017).

Although such a model may be applicable to the Quaternary Yellowstone eruptives, a distinctive signature of samples from suites 1 and 3 is their enrichment not only in typically fluid-mobile LILE (Ba, Rb) but also immobile HFSE (Zr, Ti, Nb) and REE relative to Suite 2 samples and the Absaroka volcanics (Fig. 10). In suites 1 and 3, the Ba enrichment coupled with the lack of a significant K_2O enrichment (or depletion) precludes a significant role for phlogopite while the lack of Sr enrichment precludes a significant role for carbonate in any

Always consult and cite the final, published document. See http:/www.minsocam.org or GeoscienceWorld

source enrichments, as mantle carbonates are commonly Sr enriched (Hoernle et al. 2002). These features indicate that aqueous fluids alone cannot have generated any proposed enrichment of the source zones for suites 1 and 3. However, at high pressures and temperatures (>600 °C and >0.5 GPa), HFSE, such as Zr and Ti, can be soluble in high total solute aqueous fluids or hydrous melts relative to dilute aqueous fluids (Manning et al. 2008; Hayden and Manning 2011; Wilke et al. 2012; Louvel et al. 2013, 2014). Under such circumstances HFSE may have been transported upwards from the Farallon slab to enrich the overlying mantle in HFSE. Although normally this metasomatized region would descend with the subducted plate to the deep mantle, thus causing the HFSE-depleted signature of subduction-zone volcanism (McCulloch and Gamble 1991; Louvel et al. 2013, 2014), the slowly sinking nature of the Farallon slab beneath the YSRP would mean that this HFSE-enriched zone remained in the upper mantle and became available as a source region for subsequent melting.

The geochemical signatures of suites 1 and 3 place further constraints on the nature of any fluids from the Farallon slab. The similar REE patterns between the different suites (Fig. 5) suggest that enrichment was uniform for all REE. Experimental data show that minimal REE fractionation occurs in melts when compared to aqueous fluids, suggesting that a hydrous melt was more likely the agent for HFSE enrichment (Tsay et al. 2014). Although fluids generated within the garnet stability field would have an elevated LREE/HREE ratio (Green and Adam 2003; Green et al. 2000), equilibration with spinel lherzolite lithospheric mantle melts would likely mask any deeper signature. We thus cannot preclude ascent of HFSE-enriched melts contributing to mantle enrichment from depths appropriate to the garnet stability field, but the source of the parental melts to suites 1 and 3 has to have been at levels above the garnet stability field.

Always consult and cite the final, published document. See http:/www.minsocam.org or GeoscienceWorld

The HFSE-enriched nature of suites 1 and 3 relative to the olivine tholeiites thus suggests that melting of a melt-enriched mantle source is a plausible mechanism for the generation of their parental melts. Following the 2.8 Ga magmatic/metamorphic enrichment event (inferred here and in other works from Pb isotopic signatures: Doe et al. 1982; Leeman et al. 1985), a second, Cretaceous-Eocene enrichment event has been proposed for the Absaroka Volcanic Province by Feeley (2003) and for volcanism farther east by Mirnejad and Bell (2006). We consider the possible role of this second enrichment event in our Suite 1 samples through the Sr isotopic systematics, where there is a positive correlation between $^{87}Sr/^{86}Sr$ and Rb/Sr and no apparent relationship to 1/Sr (Fig. 7). We argue (as contrasted previously for the olivine tholeiites) that this trend is not due to crustal contamination but instead controlled by Rb, which is enriched in the Suite 1 samples (Fig. 9). One interpretation for this trend, therefore, is as a pseudochron, potentially reflecting the age of the secondary Rb-enrichment event. Using age-corrected (to 2.08 Ma) $^{87}Sr/^{86}Sr$ and $^{87}Rb/^{86}Sr$ ratios, a pseudochron of 68±45 Ma (MSWD=193) is generated using Isoplot (Supplementary Fig. 7). Although imprecise, this age estimate is the same within error as that proposed for the metasomatic event associated with volcanism in the Absaroka field and elsewhere in Wyoming (Feeley 2003; Mirnejad and Bell 2006; Schmandt and Humphreys 2011). Note also that this pseudochron correlation, if valid, would indicate an original $^{87}Sr/^{86}Sr$ for the source region of the Suite 1 HRT mafics of 0.7069 ± 0.0004, identical within error to the inferred initial $^{87}Sr/^{86}Sr$ ratios of Yellowstone-Snake River Plain olivine tholeiites (0.7067 ± 0.001: McCurry and Rodgers 2009). If, in contrast, measured $^{87}Sr/^{86}Sr$ values are age-corrected to an Archean age (i.e. ≥2.5 Ga), then initial $^{87}Sr/^{86}Sr$ values would have been <0.7 and the slope of the pseudochron much steeper (Fig. 7a). This initial value is implausibly low and indicates that Rb/Sr enrichment, if related to metasomatism, did not

Always consult and cite the final, published document. See http:/www.minsocam.org or GeoscienceWorld

occur in the Archean but must be a more recent event. We consider that the younger event is recorded in Sr but not Pb isotopic systematics due to the elevated Rb/Sr in Suite 1 relative to Suite 2 samples. In contrast the U/Pb values are similar between the two suites, thus, allowing for a selective Sr isotopic overprint.

We therefore suggest that as the Farallon slab foundered in the Cretaceous-Eocene, a variety of fluids (aqueous fluids and hydrous melts) with varying compositions were released from the slab to migrate upwards into the lithospheric mantle resulting in a heterogeneous source region for subsequent melting and volcanism (Fig. 11). Aqueous fluids, enriched in LILE, likely migrated further (cf. Rubatto and Hermann 2003) and the LILE-enriched regions preferentially melted as a consequence of asthenospheric upwelling to generate the Absaroka volcanics with their high LILE/HFSE signature (Fig. 10). We infer that during subsequent impingement of the modern Yellowstone thermal anomaly (plume) the lithospheric mantle beneath the YPVF underwent partial melting. This 'modern' melting event generated parental melts for the enriched Suite 1 mafics plus Suite 3 COM-type magmas from HFSE-enriched regions, and olivine tholeiitic melts from adjacent unaltered regions that were unaltered or from which the LILE were stripped during Absaroka magmatism.

Intra-suite trends

Following generation of the parental melts, subsequent processes controlled the distinct intra-suite compositional arrays, predominantly fractional crystallization and assimilation, that we discuss in turn below. Both processes, particularly at low pressures, have been invoked for the COM-trend along the Snake River Plain (Leeman et al. 1976; Christiansen and McCurry 2008; McCurry et al. 2008). Although plagioclase and olivine are

Always consult and cite the final, published document. See http:/www.minsocam.org or GeoscienceWorld

commonly present in olivine tholeiite and COM eruptives (Putirka et al. 2009), major and trace element trends may fingerprint any other 'cryptic' fractionation effects, reflecting crystallization of phases not observed in the erupted material. Sub-parallel major element trends (e.g. increasing Na_2O + K_2O with SiO_2, and decreasing MgO, FeO and CaO) in all three suites suggest a control by similar olivine plus plagioclase fractionation assemblages (Tilley and Thompson 1970), with the additional presence of apatite to explain a decrease in P_2O_5 in suites 1 and 3, as inferred for COM flows (Fig. 3b: Leeman et al. 1976; Reid 1995). Trace element patterns, however, indicate a contrast in the relative role of fractionation of the different phases in generating the intra-suite trends. The sharp decrease in Ni/Sc ratios with decreasing MgO and CaO/Al_2O_3 in Suite 2 olivine tholeiite samples, compared to a relatively flat trend defined by suites 1 and 3, suggest a much greater role for olivine in Suite 2 samples (Supplementary Fig. 8). Conversely, the positive relationship between Sr and other LILE (e.g. Rb and Ba) in Suite 2 samples, coupled with an increase of Rb with SiO_2, indicates a bulk incompatibility of Sr and a reduced role for plagioclase (Fig. 9). This inference is supported by an increase in Sr/Sc with increasing Ni/Cr in Suite 2 samples (Supplementary Fig. 9). In contrast, samples from suites 1 and 3 show an inverse relationship between Sr and Rb (Fig. 9) and, as Rb increases with SiO_2 in all suites, these relationships collectively indicate a greater influence of plagioclase. Deviations from these trends (e.g. YR294, a Junction Butte Basalt sample with 36 ppm Rb: Fig. 9) are likely to reflect variable degrees of contamination by country rocks.

Quantitative fractional crystallization modelling was undertaken using the modeling program of Ersoy and Helvaci (2010) with their built-in partition coefficients for "basic" magmas. Starting compositions were the samples from each suite with the highest Mg# (YR291 and YR422 for suites 2 and 3 respectively) or a combination of high Mg# and low

Always consult and cite the final, published document. See http:/www.minsocam.org or GeoscienceWorld

SiO_2 (YP122: Suite 1). Results from this modeling support the previous inferences, with the Suite 2 trend most consistent with a crystallizing assemblage of 60% clinopyroxene, 35% olivine and 5% plagioclase (Fig. 9, Supplementary Fig. 9). In contrast, as shown by an antithetic evolutionary trend (Supplementary Fig. 9), the Suite 3 sample variations can be replicated by a fractional crystallization of an assemblage containing 80% plagioclase, 15% olivine and 5% clinopyroxene. This assemblage is plagioclase richer and pyroxene poorer than those observed in the experiments of Whitaker et al. (2008), conducted on a similar range of compositions. However, the model mineral assemblage and fractionation trend are at odds with the lack of a negative Eu anomaly in the Suite 3 samples (Fig. 5) as would be expected with significant plagioclase fractionation. The compositional variation of this suite is thus somewhat enigmatic and would benefit from further study. Both curves detailed above show uniform Zr/Nb ratios with changing Sr (Fig. 9), consistent with the similar incompatible nature of both elements in the fractionating assemblage.

In Suite 1 samples, although the uniform Sr/Sc ratio with decreasing Ni/Cr (Supplementary Fig. 9) is consistent with a moderately plagioclase-dominant assemblage (45% plagioclase, 30% olivine and 25% clinopyroxene), this assemblage does not fully replicate Sr, Ba and Rb trends observed in the Suite 1 data. In addition, the modeled trend is antithetic to the strong correlation between Zr/Nb and Sr observed in the sample data (Fig. 9). This correlation requires either the fractionation of zircon or a Nb-rich phases. It is possible that the decrease in Zr/Nb ratios, with decreasing Sr, is related to zircon fractionation accompanying the bulk fractionation trend, as zircon is inferred to be stable at ∼60 wt% SiO_2 in similarly Zr-rich compositions (McCurry et al. 2008). There is no petrographic evidence, however, for zircon or a Nb-rich phase being present, either in Suite 1 materials or the COM lava flows (Leeman et al. 1976). Furthermore, zircon saturation temperatures

Always consult and cite the final, published document. See http:/www.minsocam.org or GeoscienceWorld

(Watson and Harrison 1983 calibration), yield temperatures of 860-960 °C for the HRT mafics, similar to temperatures of 770-960 °C for Suite 3 samples that show constant Zr/Nb values. These are too low to be plausible pre-eruptive temperatures for these melts, particularly given that only one COM flow has yielded average plagioclase thermometry estimates of <1,000 °C (Putirka et al. 2009). We also note that Zr concentrations broadly increase in Suite 1 dense mafics across the compositional range (Fig. 4b), the opposite of what would be expected with zircon fractionation. Although Zr/Nb correlates closely with Sr contents in Suite 1 samples, Sr is scattered throughout the suite and does not show clear trends with other proxies of evolution (e.g. Rb: Fig. 9).

The large degrees of scatter in data from all three suites and the poor fit of some modelled trends (e.g. Supplementary Fig. 9), indicate that not all intra-suite trends can be explained exclusively by fractional crystallization and some crustal assimilation/mixing is also required. Although there is a rhyolite-mixing trend observed within the Suite 1 scoria samples (Fig. 4), as discussed earlier (Crustal assimilation section), this process does not explain the overall increases in Ba and Zr with SiO_2 observed in data from this suite. A diminished role for assimilation is further supported by the decoupled behavior of P_2O_5 and Zr within the Suite 1 mafics (cf. Figs. 3b, 4b), which behavior is typically attributed to fractionation rather than mixing (e.g. Lee and Bachmann 2014). Furthermore, the lack of a relationship between $^{87}Sr/^{86}Sr$ and 1/Sr (Fig. 7) in the samples from suites 1 and 3, is inconsistent with a strong assimilation control on the compositional array.

Whilst the Suite 2 samples show a large range in $^{87}Sr/^{86}Sr$ and wide ranges in incompatible elements (e.g. Rb: Fig. 9), commonly attributed to crustal assimilation (e.g. Hildreth et al. 1991; Christiansen and McCurry 2008), there are complexities to this simple model. For example, samples with Sr differing by a factor of 2 have very similar Sr isotopic

Always consult and cite the final, published document. See http:/www.minsocam.org or GeoscienceWorld

compositions and the highest-Sr lava (YR 292, Basalt of the Narrows; 546 ppm) has the lowest $^{87}Sr/^{86}Sr$ (0.70373 ± 0.00005 2se). There is also no strong correlation between $^{87}Sr/^{86}Sr$ and 1/Sr, which would be expected with significant crustal assimilation of a homogenous contaminant (Fig. 7).

Therefore, although assimilation is likely to occur in all suites, any simple explanation involving incorporation of a common assimilant is insufficient to explain the compositional arrays within each suite. The diversity within the Suite 1 samples, which is incompatible with simple fractional crystallization and assimilation models discussed above, is surprising. It is possible that variations in the suite are related to subtle differences in the degree/composition of the initial enrichment, but why any such intra-suite source variation should remain distinct during ascent through the crust and eruption is puzzling.

Comparisons and contrasts with the Craters of the Moon lava field

Our data allow us to compare our Suite 1 HRT mafics and Suite 3 local COM-type samples with their counterparts from the Craters of the Moon lava field (Leeman 1976; Putirka et al. 2009). In the first instance there are some contrasts. Suite 1 HRT mafics show relatively elevated TiO_2, Ba and Zr, and no correlation between Ba and Sr whereas Suite 3 samples and published COM data show a negative correlation (Fig. 9b). Furthermore, Suite 1 samples show a strong decrease in Zr/Nb with decreasing Sr, whereas Suite 3 samples show uniformity of Zr/Nb (Fig. 9c). Different model crystallizing assemblages (see Fig. 9 caption) yield broadly constant Zr/Nb with changing Sr, indicating that the Zr/Nb versus Sr relationships in Suite 1 samples is unlikely to be controlled by fractional crystallization. The above two features suggest that rocks of Suite 3 and the ‘type’ COM areas have signatures

Always consult and cite the final, published document. See http:/www.minsocam.org or GeoscienceWorld

that are more fractionation-controlled, whereas the Suite 1 HRT mafics have a further, enriched signature, which we relate to mantle source variations (previous section).

As previously mentioned, the COM samples reported by Putirka et al. (2009) are more radiogenic (i.e. higher $^{87}Sr/^{86}Sr$) than our samples from suites 1 and 3 which, in simple terms, reflects variations in the amount of crustal assimilation. This explanation is supported by the negative correlation between $^{143}Nd/^{144}Nd$ and $^{87}Sr/^{86}Sr$ in COM samples, forming a trend towards the average crustal isotopic composition (Fig. 6: Leeman 1976; Putirka et al. 2009). Furthermore, the initial increase in $^{87}Sr/^{86}Sr$ with Rb/Sr ratios in COM-type flows from the Craters of the Moon (Fig. 7a), starting from values similar to the least radiogenic Suite 1 HRT mafics, indicates enhanced incorporation of a more radiogenic assimilant than that inferred in the HRT mafics. The trend observed is that expected in material of Archean age (Fig. 7a), consistent with the assimilation of ancient crust in the type Craters of the Moon area.

IMPLICATIONS

Our results have a number of implications for the onset of large-scale volcanism in the Yellowstone area. The early eruption of two contrasting mafic suites (1 and 2) reflects a complex mafic root zone beneath the early Yellowstone magmatic system. Our data represent the first documentation of COM-type material associated with rhyolites within the YPVF, as all mafic rocks reported so far have been of olivine tholeiitic affinity, whether erupted close to, or outside the focus of silicic volcanism (Christiansen 2001; Christiansen and McCurry 2008; Pritchard et al. 2013). The presence of the Suite 1 HRT mafic materials indicate that genesis of such 'COM-like' magmas is more widespread than previously

Always consult and cite the final, published document. See http:/www.minsocam.org or GeoscienceWorld

thought, and that such magmas can be present at the onset of, rather than always post-dating, any focus of silicic volcanism. It also shows that a COM-like mafic lineage can also be intimately associated with large silicic eruptions, in contrast to its currently viewed association with small-scale basaltic and fractionated intermediate to silicic eruptives in the Snake River Plain (Kuntz et al. 1986; McCurry et al. 2008; Putirka et al. 2009).

The Suite 1 HRT compositions have implications for modelling of the silicic magmatism at Yellowstone. Although the HRT mafics are distinct in their elemental compositions, their isotopic compositions fall within the range of the olivine tholeiites. Any isotopic leverage on the HRT silicic system from the HRT mafic compositions is thus comparable to those from olivine tholeiites. However, the HRT mafic compositions are critical when conducting elemental modelling of the Yellowstone silicic system. The least evolved published HRT analysis has 70.8 wt% SiO_2 and 2670 ppm Ba (Hildreth et al. 1991). Our discovery of basaltic compositions (~50 wt% SiO_2) with ~2,500 ppm Ba, as opposed to ~500 ppm in the tholeiites at a similar silica content, has significant impacts when discussing petrogenesis of the least-evolved rhyolites at Yellowstone and the nature of the components involved (e.g. Christiansen and McCurry 2008).

Our study has shown a general spatial variation in the distribution of mafic components in the HRT, with dense clasts erupted with ignimbrite member A concentrated to the SW and scoria associated with upper member B concentrated to the north. Although only mafic eruptives belonging to the olivine tholeiite suite have so far been documented in the YPVF, we consider it possible that evidence for COM-type mafic contributions may be found in younger silicic deposits. However, such contributions may have been diluted out by continuing ascent of more voluminous olivine tholeiite melts. The close proximity of young eruptions of olivine tholeiite and COM-type magmas in and just west of the Island Park

Always consult and cite the final, published document. See http:/www.minsocam.org or GeoscienceWorld

segment of the HRT caldera (e.g. Christiansen 2001; Iwahashi 2010) demonstrates that these contrasting magma types do not reflect mutually exclusive magma-generating systems.

Although our Suite 2 Yellowstone olivine tholeiites represent a limited data set, it is clear that there is significant complexity within it, as well as within the broader SRP olivine tholeiite literature data. Large variations within major and trace elemental compositions (e.g. SiO_2 and Sr), and isotopic compositions (e.g. Pb and Sr isotopes) have previously been ascribed to varying degrees of contamination from crustal rocks or rhyolite melts (Hildreth et al. 1991; Christiansen and McCurry 2008). However, the lack of observed trends between elemental and isotopic compositions (e.g. Fig. 7) suggests there are further complexities than these. Furthermore, there is considerable variation within stratigraphically-grouped basalts. The multiple flow pre-HRT Junction Butte Basalt (Christiansen 2001) is considered evolved and contaminated (Hildreth et al. 1991). Although possibly the case for some flows (e.g. YR294: SiO_2 = 54.3 wt%, Rb = 36 ppm, $^{87}Sr/^{86}Sr$ = 0.70756), others show a more primitive signature (e.g. YR297: SiO_2 = 49.1 wt%, Rb = 5 ppm, $^{87}Sr/^{86}Sr$ = 0.70561). This diversity suggests that contamination processes are localized and variable, and likely involve a variety of assimilants. Consequently, we feel that the Yellowstone olivine tholeiites deserve renewed scrutiny using current compositional and geochronological capabilities to fully identify variations within the suite and the compositional role they play in the silicic magmatic system after the HRT eruption.

Although the complex compositional characteristics of the Suite 1 HRT mafics (and other COM compositions) mean there are issues with any proposed petrogenetic process (Table 4), we would argue that our proposed model of HFSE-enriched melt metasomatism in the mantle source for generation of the least-evolved melts is the most compatible with our

Always consult and cite the final, published document. See http:/www.minsocam.org or GeoscienceWorld

data. Although the generation of high P-T, HFSE-rich fluids is likely to be a common process in subduction zones (Louvel et al. 2013, 2014), causing enrichment of the overlying mantle wedge, primary enrichment is likely to be in a zone immediately overlying the subducted slab. The lower solubility HFSE elements would be likely to be precipitated first, leaving dominantly more-soluble elements (e.g. LILE) to ascend farther into the sub-continental lithospheric mantle into higher temperature regions and the focus of melting, while the HFSE-enriched zones founder with the subducted slab (Louvel et al. 2013, 2014). The unusual slab geometry beneath the YPVF, of a stationary or slowly descending slab in the asthenosphere, means that in this case the HFSE-enriched mantle, generated during Eocene and onwards foundering of the slab, has remained in the zone of potential melt generation. Therefore, with the arrival of a focused, albeit weak, thermal anomaly (the Yellowstone plume, *sensu lato*), the HFSE-enriched mantle material was located in the melting window when the lithospheric mantle was raised above its solidus at the onset of YPVF volcanism and birth of the HRT silicic system. The higher alkali contents of these metasomatized regions would also promote melting through reducing the solidus temperature (Hirschmann 2000).

It seems clear that the formation of the HRT mafics and COM-type compositions is a localized feature requiring the alignment of a variety of processes. There are additional complexities related to the local setting and conditions, particularly within the Sr isotopic signatures, between the Suite 1 HRT mafics, the Suite 3 COM-type flows analyzed here, and the more radiogenic nature of the flows from the Craters of the Moon type area (Leeman 1974; Leeman et al. 1976; Putirka et al. 2009). However, with a full major, trace and isotopic dataset we are able to offer a more consistent mechanism for generation of the parental magmas for the HRT mafic suite that may also be applicable to the broader COM suite. We

Always consult and cite the final, published document. See http:/www.minsocam.org or GeoscienceWorld

suggest that re-evaluation of the overall characteristics of the Craters of the Moon series of rocks may also be required.

Acknowledgements

Swallow is supported by a Commonwealth Scholarship administered by the Commonwealth Scholarship Commission. Wilson thanks the research offices for Yellowstone (YELL-05248) and Grand Teton (GRTE-00604) national parks for research permits and their staff for their help. Wilson also acknowledges past support from a Royal Society of New Zealand James Cook Fellowship and Marsden Fund grant VUW0813. We thank John Watson, Michael Rowe (XRF) and Sam Hammond (ICP-MS) for analytical assistance, and Julie Vry, Eugene Humphreys and Richard Carlson for useful discussions. We additionally thank Eric Christiansen and Mark Stelten for their comprehensive and informative reviews, and Erik Klemetti for editorial handling.

References

Armstrong, R.L., Leeman, W.P., and Malde, H.E. (1975) K-Ar dating, Quaternary and Neogene volcanic rocks of the Snake River Plain, Idaho. American Journal of Science, 275, 225-251.

Bachmann, O., and Bergantz, G.W., (2008) Rhyolites and their source mushes across tectonic settings. Journal of Petrology, 49, 2277-2285.

Bachmann, O., Dungan, M.A., and Lipman, P.W., (2002) The Fish Canyon magma body, San Juan volcanic field, Colorado: Rejuvenation and eruption of an upper-crustal batholith. Journal of Petrology, 43, 1469-1503.

Always consult and cite the final, published document. See http:/www.minsocam.org or GeoscienceWorld

Bacon, C.R., and Metz, J. (1984) Magmatic inclusions in rhyolites, contaminated basalts, and compositional zonation beneath the Coso volcanic field, California. Contributions to Mineralogy and Petrology, 85, 345-365.

Barker, S.J., Wilson, C.J.N., Morgan, D.J., and Rowland, J.V. (2016) Rapid priming, accumulation and recharge of magma driving recent eruptions at a hyperactive caldera volcano. Geology, 44, 323-326.

Bindeman, I.N., and Simakin, A.G. (2014) Rhyolites-Hard to produce, but easy to recycle and sequester: Integrating microgeochemical observations and numerical models. Geosphere, 10, 930-957.

Bindeman, I.N., Fu, B., Kita, N.T., and Valley, J.W. (2008) Origin and evolution of silicic magmatism at Yellowstone based on ion microprobe analysis of isotopically zoned zircons. Journal of Petrology, 49, 163-193.

Blundy, J.D., and Wood, B.J. (1991) Crystal-chemical controls on the partitioning of Sr and Ba between plagioclase feldspar, silicate melts, and hydrothermal solutions. Geochimica et Cosmochimica Acta, 55, 193-209.

Bouvier, A., Vervoort, J.D., and Patchett, P.J. (2008) The Lu-Hf and Sm-Nd isotopic composition of CHUR: Constraints from unequilibrated chondrites and implications for the bulk composition of terrestrial planets. Earth and Planetary Science Letters, 273, 48-57.

Brueseke, M.E., Downey, A.C., Dodd, Z.C., Hart, W.K., Adams, D.C., and Benowitz, J.A. (2018) The leading wisps of Yellowstone: post-ca. 5 Ma extension-related magmatism in the upper Wind River Basin, Wyoming (USA), associated with the Yellowstone hotspot tectonic parabola. Geosphere, 14 (in press, doi:10.1130/GES01553.1).

Always consult and cite the final, published document. See http:/www.minsocam.org or GeoscienceWorld

This is a preprint, the final version is subject to change, of the American Mineralogist (MSA)
Cite as Authors (Year) Title. American Mineralogist, in press.
DOI: https://doi.org/10.2138/am-2018-6273

Chadwick, R.A. (1970) Belts of eruptive centers in the Absaroka-Gallatin Volcanic Province, Wyoming-Montana. Geological Society of America Bulletin, 81, 267-274.

Charlier, B.L.A., Ginibre, C., Morgan, D., Nowell, G.M., Pearson, D.G., Davidson, J.P., and Ottley, C.J. (2006) Methods for the microsampling and high-precision analysis of strontium and rubidium isotopes at single crystal scale for petrological and geochronological applications. Chemical Geology, 232, 114-133.

Christiansen, E.H., and McCurry, M. (2008) Contrasting origins of Cenozoic silicic volcanic rocks from the western Cordillera of the United States. Bulletin of Volcanology, 70, 251-267.

Christiansen, R.L. (2001) The Quaternary and Pliocene Yellowstone Plateau volcanic field of Wyoming, Idaho, and Montana. U.S. Geological Survey Professional Paper 729-G.

Christiansen, R.L., and Yeats, R.S. (1992) Post-Laramide geology of the U.S. Cordilleran region. In B.C. Burchfield, P.W. Lipman, and M.L. Zoback, Eds., The Cordilleran orogeny: Conterminous U.S., The Geology of North America, G-3, 261-406. Geological Society of America, Boulder, Colorado.

Christiansen, R.L., Lowenstern, J.B., Smith, R.B., Heasler, H., Morgan, L.A., Nathenson, M., Mastin, L.G., Muffler, L.J.P., and Robinson, J.E. (2007) Preliminary assessment of volcanic and hydrothermal hazards in Yellowstone National Park and vicinity. U.S.G.S. Open-File Report, 2007-1071, 94 p.

Coble, M.A., and Mahood, G.A. (2012) Initial impingement of the Yellowstone plume located by widespread silicic volcanism contemporaneous with Columbia River flood basalts. Geology, 40, 655-658.

Coble, M.A., and Mahood, G.A. (2015) Geology of the High Rock caldera complex, northwest Nevada, and implications for intense rhyolitic volcanism associated with flood basalt

Always consult and cite the final, published document. See http:/www.minsocam.org or GeoscienceWorld

magmatism and the initiation of the Snake River Plain–Yellowstone trend. Geosphere, 12, 58-113.

DePaolo, D.J., and Wasserburg, G.J. (1976) Nd isotopic variations and petrogenetic models. Geophysical Research Letters, 3, 249-252.

Doe, B.R., Leeman, W.P., Christiansen, R.L., and Hedge, C.E. (1982) Lead and strontium isotopes and related trace elements as genetic tracers in the upper Cenozoic rhyolite-basalt association of the Yellowstone Plateau volcanic field. Journal of Geophysical Research, 87, 4785-4806.

Ersoy, Y., and Helvaci, C. (2010) FC-AFC-FCA and mixing modeler: a Microsoft® Excel© spreadsheet program for modeling geochemical differentiation of magma by crystal fractionation, crustal assimilation and mixing. Computers & Geosciences, 36, 383-390.

Feeley, T.C. (2003) Origin and tectonic implications of across-strike geochemical variations in the Eocene Absaroka Volcanic Province, United States. Journal of Geology, 111, 329-346.

Geist, D.J., Sims, E.N., Hughes, S.S., and McCurry, M. (2002) Open-system evolution of a single episode of Snake River Plain magmatism. In P.K. Link, and L.L. Mink, Eds., Geology, Hydrogeology and Environmental Remediation: Idaho National Engineering and Environmental Laboratory, Eastern Snake River Plain, Idaho. Geological Society of America Special Papers, 353, 193-204.

Gerstenberger, H., and Haase, G. (1996) A highly effective emitter substance for mass spectrometric Pb isotope ratio determinations. Chemical Geology, 136, 309-312.

Always consult and cite the final, published document. See http:/www.minsocam.org or GeoscienceWorld

Green, T.H., and Adam, J. (2003) Experimentally-determined trace element characteristics of aqueous fluid from partially dehydrated mafic oceanic crust at 3.0 GPa, 650-700 °C. European Journal of Mineralogy, 15, 815-830.

Green, T.H., Blundy, J.D., Adam, J., and Yaxley, G.M. (2000) SIMS determination of trace element partition coefficients between garnet, clinopyroxene and hydrous basaltic liquids at 2-7.5 GPa and 1080-1200 °C. Lithos 53, 165-187.

Hanan, B.B., Shervais, J.W., and Vetter, S.K. (2008) Yellowstone plume-continental lithosphere interaction beneath the Snake River Plain. Geology, 36, 51-54.

Hart, S.R. (1984) A large-scale isotope anomaly in the Southern Hemisphere mantle. Nature, 309, 753-757.

Hayden, L.A., and Manning, C.E. (2011) Rutile solubility in supercritical $NaAlSi_3O_8$-H_2O fluids. Chemical Geology, 284, 74-81.

Hier-Majumder, S., and Tauzin, B. (2017) Pervasive upper mantle melting beneath the western US. Earth and Planetary Science Letters, 463, 25-35.

Hildreth, W. (1981) Gradients in silicic magma chambers: Implications for lithospheric magmatism. Journal of Geophysical Research, 86, 10153-10192.

Hildreth, W., Christiansen, R.L., and O'Neil, J.R. (1984) Catastrophic isotopic modification of rhyolite magma at times of caldera subsidence, Yellowstone Plateau volcanic field. Journal of Geophysical Research, 89, 8839-8369.

Hildreth, W., Halliday, A.N., and Christiansen, R.L. (1991) Isotopic and chemical evidence concerning the genesis and contamination of basaltic and rhyolitic magma beneath the Yellowstone Plateau volcanic field. Journal of Petrology, 32, 63-138.

Hirschmann, M.M. (2000) Mantle solidus: Experimental constraints and the effects of peridotite composition. Geochemistry Geophysics Geosystems, 1, 200GC000070.

Always consult and cite the final, published document. See http:/www.minsocam.org or GeoscienceWorld

Hoernle, K., Tilton, G., Le Bas, M.J., Duggen, S., and Garbe-Schönberg, D. (2002) Geochemistry of oceanic carbonatites compared with continental carbonatites: Mantle recycling of oceanic crustal carbonate. Contributions to Mineralogy and Petrology, 142, 520-542.

Hofmann, A.W. (1988) Chemical differentiation of the Earth: The relationship between mantle, continental crust, and oceanic crust. Earth and Planetary Science Letters, 90, 297-314.

Hofmann, A.W. (1997) Mantle geochemistry: The message from oceanic volcanism. Nature, 385, 219-229.

Huang, H.-H., Lin, F.-C., Schmandt, B., Farrell, J., Smith, R.B., and Tsai, V.C. (2015) The Yellowstone magmatic system from the mantle plume to the upper crust. Science, 348, 773-776.

Huber, C., Bachmann, O., and Dufek, J. (2011) Thermo-mechanical reactivation of locked crystal mushes: Melting-induced internal fracturing and assimilation processes in magmas. Earth and Planetary Science Letters, 304, 443-454.

Hurwitz, S., and Lowenstern, J.B. (2014) Dynamics of the Yellowstone hydrothermal system. Reviews of Geophysics, 51, 375-411.

Iwahashi, G.S. (2010) Physical and compositional implications for the evolution of Spencer-High Point volcanic field, Idaho, 165 p. M.Sc. thesis, Idaho State University, Pocatello.

James, D.E., Fouch, M.J., Carlson, R.W., and Roth, J.B. (2011) Slab fragmentation, edge flow and the origin of the Yellowstone hotspot track. Earth and Planetary Science Letters, 311, 124-135.

Always consult and cite the final, published document. See http:/www.minsocam.org or GeoscienceWorld

Kuntz, M.A., Champion, D.E., Spiker, E.C., and Lefebvre, R.H. (1986) Contrasting magma types and steady-state, volume-predictable basaltic volcanism along the Great Rift, Idaho. Geological Society of America Bulletin, 97, 579-594.

Kuntz, M.A., Covington, H.R., and Schorr, L.J. (1992) An overview of basaltic volcanism of the eastern Snake River Plain, Idaho. In: P.K. Link, M.A. Kuntz, and L.B. Platt, Eds. Regional geology of eastern Idaho and western Wyoming. Geological Society of America Memoirs, 179, 227-268.

Lake, E.T., and Farmer, G.L. (2015) Oligo-Miocene mafic intrusions of the San Juan Volcanic Field, southwestern Colorado, and their relationship to voluminous, caldera-forming magmas. Geochimica et Cosmochimica Acta, 157, 86-108.

Le Bas, M.J., and Streckeisen, A.L. (1991) The IUGS systematics of igneous rocks. Journal of the Geological Society, London, 148, 825-833.

Lee, C.-T.A., and Bachmann, O. (2014) How important is the role of crystal fractionation in making intermediate magmas? Insights from Zr and P systematics. Earth and Planetary Science Letters, 393, 266-274.

Leeman, W.P. (1974) Part I: Petrology of basaltic lavas from the Snake River Plain, Idaho, and Part II: Experimental determination of partitioning of divalent cations between olivine and basaltic liquid, 337 p. Ph.D. thesis, University of Oregon, Eugene.

Leeman, W.P., and Manton, W.I. (1971) Strontium isotopic composition of basaltic lavas from the Snake River Plain, southern Idaho. Earth and Planetary Science Letters, 11, 420-434.

Leeman, W.P., Vitaliano, C.J., and Prinz, M. (1976) Evolved lavas from the Snake River Plain: Craters of the Moon National Monument, Idaho. Contributions to Mineralogy and Petrology, 56, 35-60.

Always consult and cite the final, published document. See http:/www.minsocam.org or GeoscienceWorld

Leeman, W.P., Menzies, M.A., Matty, D.J., and Embree, G.F. (1985) Strontium, neodymium and lead isotopic compositions of deep crustal xenoliths from the Snake River Plain: evidence for Archean basement. Earth and Planetary Science Letters, 75, 354-368.

Leeman, W.P., Schutt, D.L., and Hughes, S.S. (2009) Thermal structure beneath the Snake River Plain: Implications for the Yellowstone hotspot. Journal of Volcanology and Geothermal Research, 188, 57-67.

Loewen, M.W., and Bindeman, I.N. (2015) Oxygen isotope and trace element evidence for three-stage petrogenesis of the youngest episode (260-79 ka) of Yellowstone rhyolitic volcanism. Contributions to Mineralogy and Petrology, 170, 39.

Louvel, M., Sanchez-Valle, C., Malfait, W.J., Testemale, D., and Hazemann, J.-L. (2013) Zr complexation in high pressure fluids and silicate melts and implications for the mobilization of HFSE in subduction zones. Geochimica et Cosmochimica Acta, 104, 281-299.

Louvel, M., Sanchez-Valle, C., Malfait, W.J., Cardon, H., Testemale, D., and Hazemann, J.-L. (2013) Constraints on the mobilization of Zr in magmatic-hydrothermal processes in subduction zones from in situ fluid-melt partitioning experiments. American Mineralogist, 99, 1616-1625.

Manning, C.E., Wilke, M., Schmidt, C., and Cauzid, J. (2008) Rutile solubility in albite-H_2O and $Na_2Si_3O_7$-H_2O at high temperatures and pressures by in-situ synchrotron radiation micro-XRF. Earth and Planetary Science Letters, 272, 730-737.

McCulloch, M.T., and Gamble, J.A. (1991) Geochemical and geodynamical constraints on subduction zone magmatism. Earth and Planetary Science Letters, 102, 358-374.

Always consult and cite the final, published document. See http:/www.minsocam.org or GeoscienceWorld

This is a preprint, the final version is subject to change, of the American Mineralogist (MSA)
Cite as Authors (Year) Title. American Mineralogist, in press.
DOI: https://doi.org/10.2138/am-2018-6273

McCurry, M., and Rodgers, D.W. (2009) Mass transfer along the Yellowstone hotspot track I: Petrologic constraints on the volume of mantle-derived magma. Journal of Volcanology and Geothermal Research, 188, 86-98.

McCurry, M., Hayden, K.P., Morse, L.H., and Mertzman, S. (2008) Genesis of post-hotspot, A-type rhyolite of the Eastern Snake River Plain volcanic field by extreme fractional crystallization of olivine tholeiite. Bulletin of Volcanology, 70, 361-383.

McDonough, W.F., and Sun, S.-s. (1995) The composition of the Earth. Chemical Geology, 120, 223-253.

McGee, L.E., Smith, I.E.M., Millet, M.-A., Handley, H.K., and Lindsay, J.M. (2013) Asthenospheric control of melting processes in a monogenetic basaltic system: A case study of the Auckland volcanic field, New Zealand. Journal of Petrology, 54, 2125-2153.

Menzies, M.A., Leeman, W.P., and Hawkesworth, C.J. (1984) Geochemical and isotopic evidence for the origin of continental flood basalts with particular reference to the Snake River Plain, Idaho, U.S.A. Philosophical Transactions of the Royal Society of London, A310, 643-660.

Mirnejad, H., and Bell, K. (2006) Origin and source evolution of the Leucite Hills lamproites: evidence from Sr-Nd-Pb-O isotopic compositions. Journal of Petrology, 47, 2463-2489.

Pierce, K.L., and Morgan, L.A. (1992) The track of the Yellowstone hot spot: Volcanism, faulting, and uplift. In: P.K. Link, M.A. Kuntz, and L.B. Platt, Eds. Regional geology of eastern Idaho and western Wyoming. Geological Society of America Memoirs, 179, 1-53.

Always consult and cite the final, published document. See http:/www.minsocam.org or GeoscienceWorld

Pierce, K.L., and Morgan, L.A. (2009) Is the track of the Yellowstone hotspot driven by a deep mantle plume? – Review of volcanism, faulting, and uplift in light of new data. Journal of Volcanology and Geothermal Research, 188, 1-25.

Pin, C., Gannoun, A., and Dupont, A. (2014) Rapid, simultaneous separation of Sr, Pb, and Nd by extraction chromatography prior to isotope ratios determination by TIMS and MC-ICP-MS. Journal of Analytical Atomic Spectrometry, 29, 1858-1870.

Pritchard, C.J., Larson, P.B., Spell, T.L., and Tarbert, K.D. (2013) Eruption-triggered mixing of extra-caldera basalt and rhyolite complexes along the East Gallatin-Washburn fault zone, Yellowstone National Park, WY, USA. Lithos, 175-176, 163-177.

Putirka, K.D., Kuntz, M.A., Unruh, D.M., and Vaid, N. (2009) Magma evolution and ascent at the Craters of the Moon and neighboring volcanic fields, southern Idaho, USA: Implications for the evolution of polygenetic and monogenetic volcanic fields. Journal of Petrology, 50, 1639-1665.

Ramsey, M.H., Potts, P.J., Webb, P.C., Watkins, P., Watson, J.S., and Coles, B.J. (1995) An objective assessment of analytical method precision: comparison of ICP-AES and XRF for the analysis of silicate rocks. Chemical Geology, 124, 1-19.

Rasoazanamparany, C., Widom, E., Valentine, G.A., Smith, E.I., Cortés, J.A., Kuentz, D., and Johnsen, R. (2015) Origin of chemical and isotopic heterogeneity in a mafic, monogenetic volcanic field: A case study of the Lunar Crater Volcanic Field, Nevada. Chemical Geology, 397, 76-93.

Reid, M.R. (1995) Processes of mantle enrichment and magmatic differentiation in the eastern Snake River Plain: Th isotope evidence. Earth and Planetary Science Letters, 131, 239-254.

Always consult and cite the final, published document. See http:/www.minsocam.org or GeoscienceWorld

This is a preprint, the final version is subject to change, of the American Mineralogist (MSA)
Cite as Authors (Year) Title. American Mineralogist, in press.
DOI: https://doi.org/10.2138/am-2018-6273

Rivera, T.A., Schmitz, M.D., Crowley, J.L., and Storey, M. (2014) Rapid magma evolution constrained by zircon petrochronology and $^{40}Ar/^{39}Ar$ sanidine ages for the Huckleberry Ridge Tuff, Yellowstone, USA. Geology, 42, 643-646.

Rosman, K.J.R., and Taylor, P.D.P. (1998) Isotopic compositions of the elements 1997. Pure and Applied Chemistry, 70, 217-235.

Rubatto, D., and Hermann, J. (2003) Zircon formation during fluid circulation in eclogites (Monviso, Western Alps): Implications for Zr and Hf budget in subduction zones. Geochimica et Cosmochimica Acta, 67, 2173-2187.

Schmandt, B., and Humphreys, E. (2010) Complex subduction and small-scale convection revealed by body-wave tomography of the western United States upper mantle. Earth and Planetary Science Letters, 297, 435-445.

Schmandt, B., and Humphreys, E. (2011) Seismically imaged relict slab from the 55 Ma Siletzia accretion to the northwest United States. Geology, 39, 175-178.

Schmandt, B., Dueker, K., Humphreys, E., and Hansen, S. (2012) Hot mantle upwelling across the 660 beneath Yellowstone. Earth and Planetary Science Letters, 331-332, 224-236.

Singer, B.S., Jicha, B.R., Condon, D.J., Macho, A.S., Hoffman, K.A., Dierkhising, J., Brown, M.C., Feinberg, J.M., and Kidane, T. (2014) Precise ages of the Réunion event and Huckleberry Ridge excursion: Episodic clustering of geomagnetic instabilities and the dynamics of flow within the outer core. Earth and Planetary Science Letters, 405, 25-38.

Singer, B.S., Costa, F., Herrin, J.S., Hildreth, W., and Fierstein, J. (2016) The timing of compositionally-zoned magma reservoirs and mafic ‘priming’ weeks before the 1912 Novarupta-Katmai rhyolite eruption. Earth and Planetary Science Letters, 451, 125-137.

Always consult and cite the final, published document. See http:/www.minsocam.org or GeoscienceWorld

Smith, R.B., Jordan, M., Steinberger, B., Puskas, C.M., Farrell, J., Waite, G.P., Husen, S., Chang, W.-L., and O'Connell, R. (2009) Geodynamics of the Yellowstone hotspot and mantle plume: Seismic and GPS imaging, kinematics, and mantle flow. Journal of Volcanology and Geothermal Research, 188, 26-56.

Sparks, R.S.J., Sigurdsson, H., and Wilson, L. (1977) Magma mixing: a mechanism for triggering acid explosive eruptions. Nature, 267, 315-318.

Stelten, M.E., Cooper, K.M., Wimpenny, J.B., Vazquez, J.A., and Yin, Q.-Z. (2017) The role of mantle-derived magmas in the isotopic evolution of Yellowstone's magmatic system. Geochemistry, Geophysics, Geosystems, 18, 1350-1365.

Sun, C., Graff, M., and Liang, Y. (2017) Trace element partitioning between plagioclase and silicate melt: The importance of temperature and plagioclase composition, with implications for terrestrial and lunar magmatism. Geochimica et Cosmochimica Acta, 206, 273-295.

Sun, S.-s., and McDonough, W.F. (1989) Chemical and isotopic systematics of oceanic basalts: Implications for mantle composition and processes. Geological Society of London Special Publications, 42, 313-345.

Thirlwall, M.F. (1991) Long-term reproducibility of multicollector Sr and Nd isotope ratio analysis. Chemical Geology, 94, 85-104.

Thirlwall, M.F. (2000) Inter-laboratory and other errors in Pb isotope analyses investigated using a ^{207}Pb-^{204}Pb double spike. Chemical Geology, 163, 299-322.

Thompson, R.N. (1975) Primary basalts and magma genesis II. Snake River Plain, Idaho, U.S.A. Contributions to Mineralogy and Petrology, 52, 213-232.

Tilley, C.E., and Thompson, R.N. (1970) Melting and crystallization relations of the Snake River basalts of southern Idaho, USA. Earth and Planetary Science Letters, 8, 79-92.

Always consult and cite the final, published document. See http:/www.minsocam.org or GeoscienceWorld

Todt, W., Cliff, R.A., Hanser, A., and Hofmann, A.W. (1996) Evaluation of a ^{202}Pb-^{205}Pb double spike for high-precision lead isotope analysis. In A. Basu, and S. Hart, Eds., Earth Processes: Reading the Isotopic Code, 95, p. 429-437. Geophysical Monographs, American Geophysical Union, Washington, D.C.

Tsay, A., Zajacz, Z., and Sanchez-Valle, C. (2014) Efficient mobilization and fractionation of rare-earth elements by aqueous fluids upon slab dehydration. Earth and Planetary Science Letters, 398, 101-112.

Watson, E.B., and Harrison, T.M. (1983) Zircon saturation revisited: temperature and composition effects in a variety of crustal magma types. Earth and Planetary Science Letters, 64, 295-304.

Whitaker, M.L., Nekvasil, H., Lindsley, D.H., and McCurry, M. (2008) Can crystallization of olivine tholeiite give rise to potassic rhyolites?—an experimental investigation. Bulletin of Volcanology, 70, 417-434.

Wilcox, R.E. (1944) Rhyolite-basalt complex on Gardiner River, Yellowstone Park, Wyoming. Geological Society of America Bulletin, 55, 1047-1080.

Wilke, M., Schmidt, C., Dubrail, J., Appel, K., Borchert, M., Kvashnina, K., and Manning, C.E. (2012) Zircon solubility and zirconium complexation in H_2O+Na_2O+SiO_2±Al_2O_3 fluids at high pressure and temperature. Earth and Planetary Science Letters, 349-350, 15-25.

Wilson, C.J.N., Blake, S., Charlier, B.L.A., and Sutton, A.N. (2006) The 26.5 ka Oruanui eruption, Taupo volcano, New Zealand: development, characteristics and evacuation of a large rhyolitic magma body. Journal of Petrology, 47, 35-69.

Always consult and cite the final, published document. See http:/www.minsocam.org or GeoscienceWorld

This is a preprint, the final version is subject to change, of the American Mineralogist (MSA)
Cite as Authors (Year) Title. American Mineralogist, in press.
DOI: https://doi.org/10.2138/am-2018-6273

Wotzlaw, J.-F., Bindeman, I.N., Stern, R.A., D'Abzac, F.-X., and Schaltegger, U. (2015) Rapid heterogeneous assembly of multiple magma reservoirs prior to Yellowstone supereruptions. Scientific Reports, 5, 14026.

Yuan, H., and Dueker, K. (2005) Teleseismic P-wave tomogram of the Yellowstone plume. Geophysical Research Letters, 32, L07304.

Zhou, Q., Liu, L., and Hu, J. (2018) Western US volcanism due to intruding oceanic mantle driven by ancient Farallon slabs. Nature Geoscience, 11, 70-76.

Zindler, A., and Hart, S. (1986) Chemical geodynamics. Annual Review of Earth and Planetary Sciences, 14, 493-571.

Figure Captions

Figure 1: Map of the Yellowstone- Snake River Plain area (adapted from Kuntz et al. 1982 and Christiansen et al. 2007). Within the Yellowstone Plateau volcanic field, the red line marks the mapped rim of the caldera for the Huckleberry Ridge Tuff (HRT) eruption, and the location of the pre-HRT Junction Butte Basalt (JBB) is also shown (from Christiansen 2001). Quaternary basaltic lava fields along the Snake River Plain (SRP) are also outlined, including those of olivine tholeiitic affinity (purple; SH-Shoshone, W-Wapi, KB-King's Bowl, NR-North Robbers, SR-South Robbers, CG-Cerro Grande, HHA-Hells Half Acre) and those containing Craters of the Moon-type magmas (orange; COM-Craters of the Moon, SHP-Spencer-High Point). The 85 km Great Rift (GR) and the boundary of Yellowstone National Park (YNP) are also shown for reference.

Figure 2: Photographs of representative HRT dense mafic (top) and scoria (bottom) clasts found dominantly in HRT members A and B, respectively. The crenulated margin of the HRT dense mafic clast indicates its juvenile nature.

Always consult and cite the final, published document. See http:/www.minsocam.org or GeoscienceWorld

This is a preprint, the final version is subject to change, of the American Mineralogist (MSA)
Cite as Authors (Year) Title. American Mineralogist, in press.
DOI: https://doi.org/10.2138/am-2018-6273

Figure 3: SiO_2 versus (a) total alkalis and b) P_2O_5 for the three suites of mafic samples analyzed in this study and relevant compositional fields from published data (see text for details). Although there is overlap between the alkali compositions of the mafic suites, P_2O_5 compositions are distinctly higher in the Suite 1 HRT samples. M denotes mingled clasts (YP185 and YP188 discussed in the text). Classification fields in panel (a) are from Le Bas and Streckeisen (1991). 2sd uncertainties are smaller than the symbol sizes.

Figure 4: Compositional diagrams for the samples analyzed in this study and relevant compositional fields from published data for SiO_2 versus (a) Ba and (b) Zr, showing the enrichment in both LILE and HFSE in samples from suites 1 and 3. HRT dense mafics and scoria (Suite 1) are further enriched in Ba relative to COM-type flows, including our Suite 3 samples. See text for sources of published data fields. A possible mixing trend with rhyolite is defined by the scoria samples, trending towards the mingled clast (M). 2sd uncertainties are smaller than the symbol size.

Figure 5: Chondrite-normalized (McDonough and Sun 1995) REE plot showing enriched but sub-parallel trends in the samples from suites 1 and 3 relative to Suite 2. There is no significant Eu anomaly in any of the samples analyzed in this study.

Figure 6: $^{143}Nd/^{144}Nd$ versus $^{87}Sr/^{86}Sr$ (age corrected) for samples analyzed in this study and isotopic fields for relevant comparators from the YSRP area (see text for published data sources). All of the samples analyzed in this study fall within the field covered by Snake River Plain basalts. The radiogenic nature of the Sr isotopic systematics, and unradiogenic Nd isotopic compositions, is taken to indicate interaction of the mafic suites with Archean subcontinental lithospheric mantle (Hanan et al. 2008). Arrow indicates trend of evolved lava flows from Craters of the Moon (Putirka et al.

Always consult and cite the final, published document. See http:/www.minsocam.org or GeoscienceWorld

This is a preprint, the final version is subject to change, of the American Mineralogist (MSA)
Cite as Authors (Year) Title. American Mineralogist, in press.
DOI: https://doi.org/10.2138/am-2018-6273

2009) towards average continental crust ($^{87}Sr/^{86}Sr$ = 0.72; $^{143}Nd/^{144}Nd$ = 0.5118: Hofmann 1997). Black asterisk represents the focus of collated Yellowstone-Snake River Plain basalts ($^{87}Sr/^{86}Sr$ = 0.7067, $^{143}Nd/^{144}Nd$ = 0.510245: McCurry and Rodgers 2009). Archean crust typically has ε_{Nd} -<15 (McCurry and Rodgers 2009, and references therein). Approximate values for enriched mantle 1 (EM2) and 2 (EM2) from Zindler and Hart (1986). See text for explanation of ε_{Nd}. 2se errors are smaller than the symbol size.

Figure 7: Plots showing the relationship between elemental and isotopic Sr compositions. Age-corrected $^{87}Sr/^{86}Sr$ values versus (a) Rb/Sr and (b) 1/Sr show a positive relationship between $^{87}Sr/^{86}Sr$ and Rb/Sr for the Suite 1 HRT mafics (R^2 = 0.65) but no clear relationship with 1/Sr. Suite 2 olivine tholeiite samples analyzed for this study show a large range in isotopic compositions with a minimal range in Rb/Sr. See text for published data sources. Vectors show modelled gradients for hypothetical Rb/Sr enrichment events at 2.77 Ga and 68 Ma from a common initial $^{87}Sr/^{86}Sr$ and multiple initial Rb/Sr ratios. 2se error bars ($^{87}Sr/^{86}Sr$) are smaller than the symbols.

Figure 8: Pb-isotopic compositions for the samples analyzed for this study and fields for published data (see text for published data sources). All samples, except for the Basalt of the Narrows (YR292) in panel (a), plot above the Northern Hemisphere reference line (NHRL: Hart 1984). Suite 1 HRT mafics show elevated $^{207}Pb/^{204}Pb$ and $^{208}Pb/^{204}Pb$ ratios for a given value of $^{206}Pb/^{204}Pb$ relative to the Suite 2 olivine tholeiites. Enriched mantle 1 (EM1) and 2 (EM2) and depleted mantle (DMM) values from Zindler and Hart (1986). Individual 2se errors are smaller than the symbol size unless indicated otherwise.

Always consult and cite the final, published document. See http:/www.minsocam.org or GeoscienceWorld

This is a preprint, the final version is subject to change, of the American Mineralogist (MSA)
Cite as Authors (Year) Title. American Mineralogist, in press.
DOI: https://doi.org/10.2138/am-2018-6273

Figure 9: Sr vs (a) Rb, (b) Ba and (c) Zr/Nb for samples analyzed in this work. Suite 1 HRT mafics are differentiated from Suite 3 COM samples by their elevated Ba and no correlation with Sr, (panel b) and strongly decreasing Zr/Nb (panel c), the latter which requires crystallization of zircon or a Nb-rich phase, both of which are unlikely to have been present. Note the positive correlation between Sr and other LILE in Suite 2 olivine tholeiite samples, indicating the incompatibility of Sr in these samples despite the presence of plagioclase. Red, purple and orange dashed lines show modelled fractional crystallization trends for Suite 1 (YP122 as starting composition, crystallizing assemblage of 45% plagioclase, 30% olivine, 25% clinopyroxene), Suite 2 (YR291 as starting composition, crystallizing assemblage of 60% clinopyroxene, 35% olivine, 5% plagioclase) and Suite 3 (YR422 as starting composition, crystallizing assemblage of 80% plagioclase, 15% olivine, 5% clinopyroxene), respectively. Modelling was done using the modeler from Ersoy and Helvaci (2010). Black crosses represent 9% increments of crystallization. Suite 1 samples have Zr/Nb ratios not consistent with a fractionation control. Suite 2 and 3 samples are consistent with an clinopyroxene- and plagioclase-dominated fractionation signature respectively, suggested by antithetic behavior of Sr with increasing Ba (panel b) and uniformity in Zr/Nb (panel c). See text for sources of published data. M denotes mingled scoria clast YP188.

Figure 10: Ocean Island Basalt-normalized (Sun and McDonough 1989) multi-element diagram showing the enriched nature in LILE and HFSE of the Suite 1 HRT mafics and Suite 3 COM-type materials relative to Suite 2 olivine tholeiites. Absaroka Volcanic Province data from Feeley (2003) show a high LILE/HFSE ratio typical of hydrous fluid-enriched subduction zone volcanism.

Always consult and cite the final, published document. See http:/www.minsocam.org or GeoscienceWorld

This is a preprint, the final version is subject to change, of the American Mineralogist (MSA)
Cite as Authors (Year) Title. American Mineralogist, in press.
DOI: https://doi.org/10.2138/am-2018-6273

Figure 11: Summary cartoon showing our proposed late Cretaceous-Eocene enrichment of the lithospheric mantle beneath Yellowstone by fluids derived from the subducted and foundering Farallon slab. Aqueous fluids with high LILE/HFSE ratios ascended and enriched the source region of the Eocene Absaroka Volcanic Province. Contemporaneously, solute-rich, LILE plus HFSE-enriched hydrous melts ascended into the base of the lithospheric mantle. Aqueous fluid enriched regions preferentially melted during asthenospheric upwelling to generate the Absaroka Volcanic Province. The renewal of volcanism in the YPVF in the Quaternary, with the arrival of a thermal anomaly (the Yellowstone plume), melted the heterogeneous lithospheric mantle. Unaltered regions yielded the parental melts to the olivine tholeiites (Suite 2, e.g. the Junction Butte Basalt) and enriched zones yielded the parental melts to the Suite 1 HRT mafics. The latter ascended to be intercepted by the growing HRT silicic magma system, syn-eruptively in the case of the samples analyzed here. Younger COM-type lavas erupted immediately west of the HRT caldera (Suite 3) also show evidence for derivation from a HFSE-enriched source.

Always consult and cite the final, published document. See http:/www.minsocam.org or GeoscienceWorld

This is a preprint, the final version is subject to change, of the American Mineralogist (MSA)
Cite as Authors (Year) Title. American Mineralogist, in press.
DOI: https://doi.org/10.2138/am-2018-6273

Table 1. Summary of the sample suites analyzed for this study.

Sample group	Host unit	Characteristics
Suite 1: dense mafics	HRT member A and rarely in member B	Small (<10 cm), dense, rounded, grey-green (rarely oxidised red) clasts often with a crenulated margin indicating a juvenile nature (Fig. 2a). Commonly aphyric (devitrified) with rare sparsely porphyritic samples containing euhedral feldspars.
Suite 1: scoria	Top of HRT member B	Black, or purple-red (where oxidised), aphyric, moderately vesicular material which occurs as discrete clasts or streaks within rhyolitic pumice. Where mingled in pumice, the scoria often includes up to 1 cm feldspar xenocrysts derived from the host pumice (Fig. 2b).
Suite 2: Snake River Plain olivine tholeiites	Pre and post HRT olivine tholeiites lava flows (Christiansen 2001)	Aphyric to sparsely porphyritic lava flows with olivine and plagioclase dominant mineral assemblages.
Suite 3: COM eruptives	Spencer-High Point (SHP) volcanic field (Iwahashi 2010)	Black-red scoriaceous bombs and lava flows (only pyroclastic material sampled). Ranges in crystallinity from 0-15%. Porphyritic crystal-rich materials contain euhedral feldspars up to 2 cm in length.

Always consult and cite the final, published document. See http:/www.minsocam.org or GeoscienceWorld

	Sample	Host unit	SiO_2	TiO_2	FeO	MgO	CaO	Na_2O	K_2O	P_2O_5	Mg#	Sc	V	Cr	Ni	Rb	Sr	Zr	Nb	Ba	La	Yb	Hf	U
Suite 1	YP122	HRT A Dense mafic	50.79	3.00	14.22	2.42	7.24	3.32	1.80	1.52	23	36	132	5.1	5.8	46	340	1575	29	2863	95	10.1	26	1.7
	YP244	HRT A Dense mafic	59.50	2.09	10.46	0.60	4.12	3.62	2.97	1.09	9	21	69	5.9	6.0	63	247	1386	43	3508	76	5.8	26	2.6
	YP246	HRT A Dense mafic	58.10	2.51	9.58	0.83	4.94	3.84	2.92	1.39	13	25	107	5.3	5.2	61	269	1099	58	2641	85	6.2	22	2.4
	YP449	HRT A Dense mafic	52.28	3.47	13.10	0.74	5.66	3.26	2.23	1.69	9	43	121	21.2	4.7	46	342	1828	40	3430	142	9.9	33	2.1
	YP071 BLACK	HRT B Scoria	55.08	2.20	12.46	2.52	6.03	3.39	2.40	1.12	27	29	88	5.2	5.4	54	277	1545	37	3802	59	6.6	28	2.2
	YP266 SCORIA	HRT B Scoria	57.98	1.94	11.10	2.19	5.21	2.90	2.95	0.97	26	24	76	2.8	5.0	67	247	1266	39	3358	67	6.3	23	2.5
	YP334B	HRT B Scoria	56.79	2.03	11.50	2.36	5.40	3.41	2.90	1.00	27	26	80	5.4	5.2	68	265	1353	39	3530	72	6.6	26	2.6
Suite 2	YR291	Warm River Basalt	47.18	1.20	10.71	10.77	10.70	2.19	0.21	0.19	64	22	241	538	190	3.1	152	77	17	120	6.3	1.3	1.9	0.1
	YR292	Basalt of the Narrows	49.39	1.91	10.35	6.68	8.48	3.30	1.15	0.36	53	20	223	48	44	22	546	172	33	423	26	1.5	3.9	0.6
	YR294	Junction Butte Basalt	54.28	1.94	10.24	4.24	7.68	3.06	1.62	0.41	42	20	213	20	26	36	366	236	19	641	30	2.1	5.4	0.9
	YR297	Junction Butte Basalt	49.09	1.92	11.45	6.90	9.97	2.65	0.40	0.23	52	17	258	65	83	5.2	320	146	12	168	9.0	1.2	3.6	0.2
	YR302	Gerrit Basalt	46.39	1.96	12.63	7.67	10.02	2.74	0.27	0.30	52	21	278	101	104	2.1	250	137	10	174	8.9	1.3	3.2	0.2
Suite 3	YR305	High Point scoria cone	56.53	1.31	10.72	1.55	4.74	4.28	3.35	0.60	20	19	2.8	37	1.0	58	185	1973	87	2185	63	8.1	36	3.5
	YR418	Un-named scoria cone	50.19	2.47	13.71	3.09	6.58	3.69	2.30	1.61	29	24	68	11	2.2	65	234	1089	83	1716	107	9.2	20	2.2
	YR420	Un-named scoria cone	50.53	2.45	13.62	3.07	6.49	3.58	2.33	1.58	29	25	73	3.2	2.4	70	245	1182	87	1814	114	9.2	22	2.3
	YR425	Blacks Knoll	47.26	3.01	14.13	3.72	8.01	3.79	1.57	2.20	32	23	104	2.9	3.3	34	347	753	61	1262	92	7.7	14	1.3

Table 2: Major and trace element analyses of selected samples from each of the suites in this study. Oxides are in wt% and elemental concentrations in ppm. Full data set can be found in Electronic Appendix 1.

Always consult and cite the final, published document. See http:/www.minsocam.org or GeoscienceWorld

This is a preprint, the final version is subject to change, of the American Mineralogist (MSA)
Cite as Authors (Year) Title. American Mineralogist, in press.
DOI: https://doi.org/10.2138/am-2018-6273

	Sample	Host unit	$^{87}Sr/^{86}Sr$	2se	$^{143}Nd/^{144}Nd$	2se	$^{206}Pb/^{204}Pb$	2se	$^{207}Pb/^{204}Pb$	2se	$^{208}Pb/^{204}Pb$	2se
Suite 1	YP122	HRT A Dense mafic	0.70721	3.69E-06	0.51231	2.79E-06	16.952	2.75E-03	15.445	3.65E-03	37.919	1.18E-02
	YP244	HRT A Dense mafic	0.70754	3.43E-06	0.51229	6.18E-06	16.892	1.12E-03	15.463	1.37E-03	37.943	4.28E-03
	YP246	HRT A Dense mafic	0.70728	3.57E-06	0.51232	4.73E-06	16.878	9.26E-04	15.458	9.98E-04	37.925	2.92E-03
	YP449	HRT A Dense mafic	0.70731	3.94E-06	0.51229	3.84E-06	16.882	9.26E-04	15.461	1.05E-03	37.937	3.18E-03
	YP071BLACK	HRT B Scoria	0.70751	3.46E-06	0.51235	5.15E-06	16.968	1.98E-03	15.481	2.55E-03	38.028	8.17E-03
	YP266SCORIA	HRT B Scoria	0.70771	3.63E-06	0.51231	2.42E-06	16.947	7.74E-04	15.476	8.22E-04	38.016	2.36E-03
	YP334B	HRT B Scoria	0.70769	3.76E-06	0.51232	4.10E-06	16.978	1.07E-03	15.482	1.24E-03	38.023	3.79E-03
Suite 2	YR291	Warm River Basalt	0.70604	3.13E-06	0.51244	3.82E-06	17.309	2.41E-03	15.511	2.35E-03	38.233	6.31E-03
	YR292	Basalt of the Narrows	0.70373	5.03E-06	0.51251	4.81E-06	16.665	3.35E-03	15.297	4.55E-03	36.466	1.44E-02
	YR294	Junction Butte Basalt	0.70756	3.87E-06	0.51207	3.71E-06	15.859	1.68E-03	15.272	2.26E-03	36.782	7.05E-03
	YR297	Junction Butte Basalt	0.70561	3.89E-06	0.51251	4.03E-06	16.943	1.27E-03	15.415	1.32E-03	37.505	3.68E-03
	YR302	Gerrit Basalt	0.70808	3.81E-06	0.51244	4.25E-06	17.031	2.04E-03	15.478	2.62E-03	37.811	8.32E-03
Suite 3	YR305	High Point scoria cone	0.70577	3.66E-06	0.51239	5.56E-06	17.218	1.06E-03	15.479	1.28E-03	38.142	3.97E-03
	YR418	Un-named scoria cone	0.70581	3.70E-06	0.51239	3.25E-06	17.208	1.36E-03	15.476	1.34E-03	38.131	3.71E-03
	YR420	Un-named scoria cone	0.70588	3.56E-06	0.51240	2.65E-06	17.158	1.10E-03	15.479	1.05E-03	38.150	2.82E-03
	YR425	Blacks Knoll	0.70789	4.43E-06	0.51225	3.32E-06	17.361	5.73E-03	15.507	5.28E-03	38.069	1.34E-02

Table 3: Isotopic ratios from selected samples from each of the suites in this study.

Always consult and cite the final, published document. See http:/www.minsocam.org or GeoscienceWorld

DOI: https://doi.org/10.2138/am-2018-6273

Process	Evidence for	Evidence against
Extreme fractional crystallization of an olivine tholeiitic parent magma	Using $\overline{D}$ = 0 for selected trace elements (e.g. Ba, Zr, U), >80% crystallization required to generate Suite 1 compositions. Similar amount to experimentally-determined degree required to generate liquids with similar major element characteristics to a COM from a tholeiitic parent (Whitaker et al. 2008)	Similar Sr concentrations between the olivine tholeiite and HRT/COM suites and absence of an Eu anomaly in suites 1 and 3 which would be expected from plagioclase dominated fractionation
Crustal assimilation	Elevated $^{87}Sr/^{86}Sr$ isotopic ratios in suites 1 and 3, and particularly in published data from the Craters of the Moon lava field (Leeman 1976; Putirka et al. 2009)	Absence of a viable assimilant in databases with high Ba, Zr and FeO, moderate K_2O and Sr, and with a flat REE pattern. Comparable $^{87}Sr/^{86}Sr$ between the different mafic suites and lack of a strong relationship between $^{87}Sr/^{86}Sr$ and 1/Sr, which would be expected with assimilation
Depth of melting	Elevated HREE concentrations in the suites 1 and 3 apparently rules out residual garnet in the source	Similar $(Gd/Yb)_N$ between the different suites indicating similar depths of equilibration for suite 1 and 3 melts to the olivine tholeiites that equilibrated with spinel lherzolite lithospheric mantle (Leeman et al. 2009)
Degree of melting	Incompatible element enrichment favours small degree of partial melting	Negative correlation between Nb/Zr and Ba/Nb in Suite 1 samples. Different degrees of partial melting would generate a positive trend due to relative degrees of incompatibility (Ba > Nb > Zr).
Aqueous fluid enrichment	Enrichment of LILE and mechanism invoked for Eocene regional volcanism due to dehydration of underlying Farallon slab (Feeley 2003)	Enrichment in aqueous fluid immobile HFSE (e.g. Zr, Ti) in suites 1 and 3, resulting in similar LILE/HFSE ratios in the mafic suites, and lack of significant K_2O enrichment in suites 1 and 3
Hydrous melt enrichment	Enrichment in LILE and HFSE in suites 1 and 3, and parallel REE patterns between the mafic suites, with enrichment in all REE aided by hydrous melts (Tsay et al. 2014)	Localised nature of enrichment and significantly different characteristics to contemporaneously derived aqueous fluids

Table 4: Summary of the possible end-member processes for generation of the parental melt to the Suite 1 HRT mafics, together with respective evidence for or against the relevant process. See text for further discussion.

Always consult and cite the final, published document. See http:/www.minsocam.org or GeoscienceWorld

This is a preprint, the final version is subject to change, of the American Mineralogist (MSA)
Cite as Authors (Year) Title. American Mineralogist, in press.
DOI: https://doi.org/10.2138/am-2018-6273

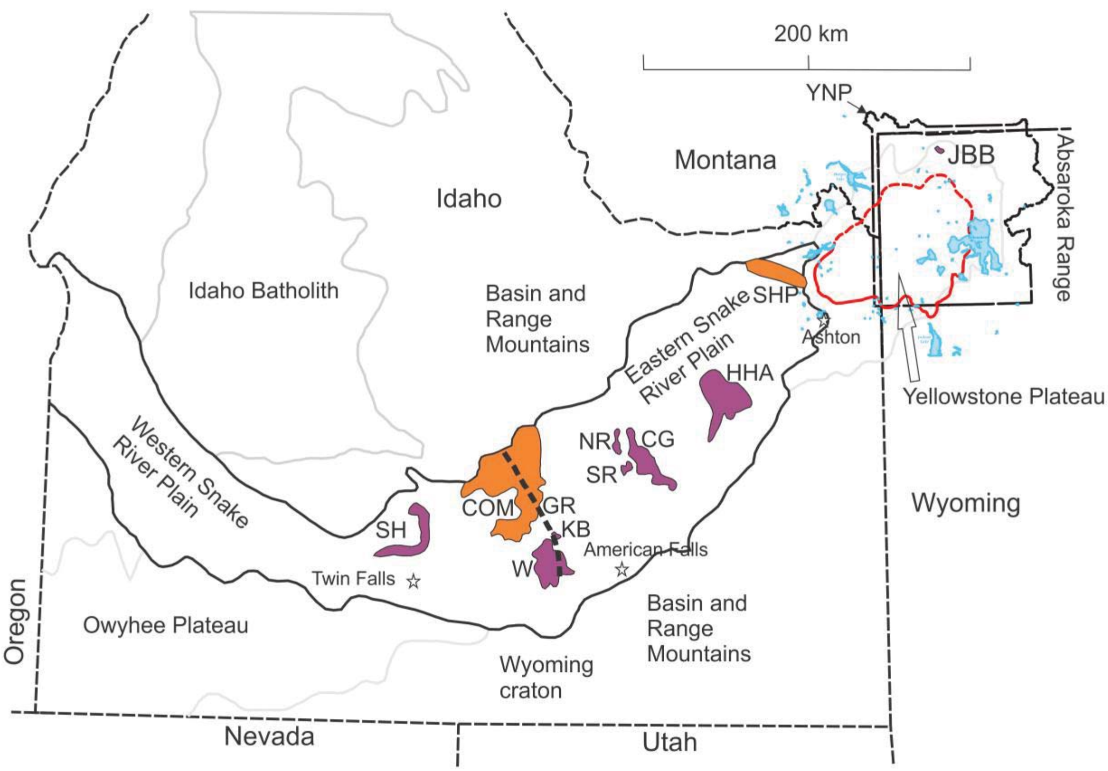

Figure 1

Always consult and cite the final, published document. See http:/www.minsocam.org or GeoscienceWorld

DOI: https://doi.org/10.2138/am-2018-6273

Figure 2

Always consult and cite the final, published document. See http:/www.minsocam.org or GeoscienceWorld

DOI: https://doi.org/10.2138/am-2018-6273

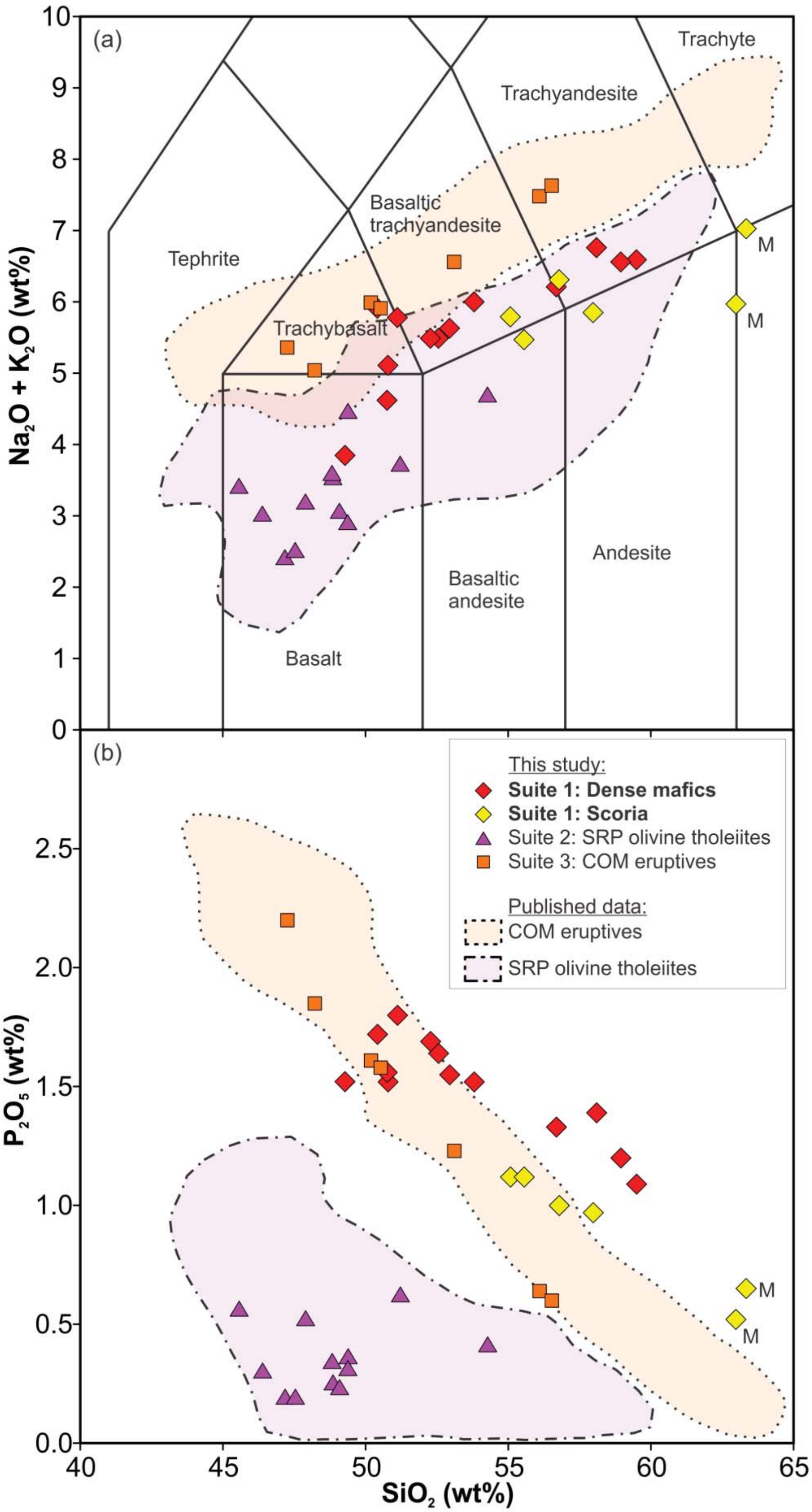

Figure 3

This is a preprint, the final version is subject to change, of the American Mineralogist (MSA)
Cite as Authors (Year) Title. American Mineralogist, in press.
DOI: https://doi.org/10.2138/am-2018-6273

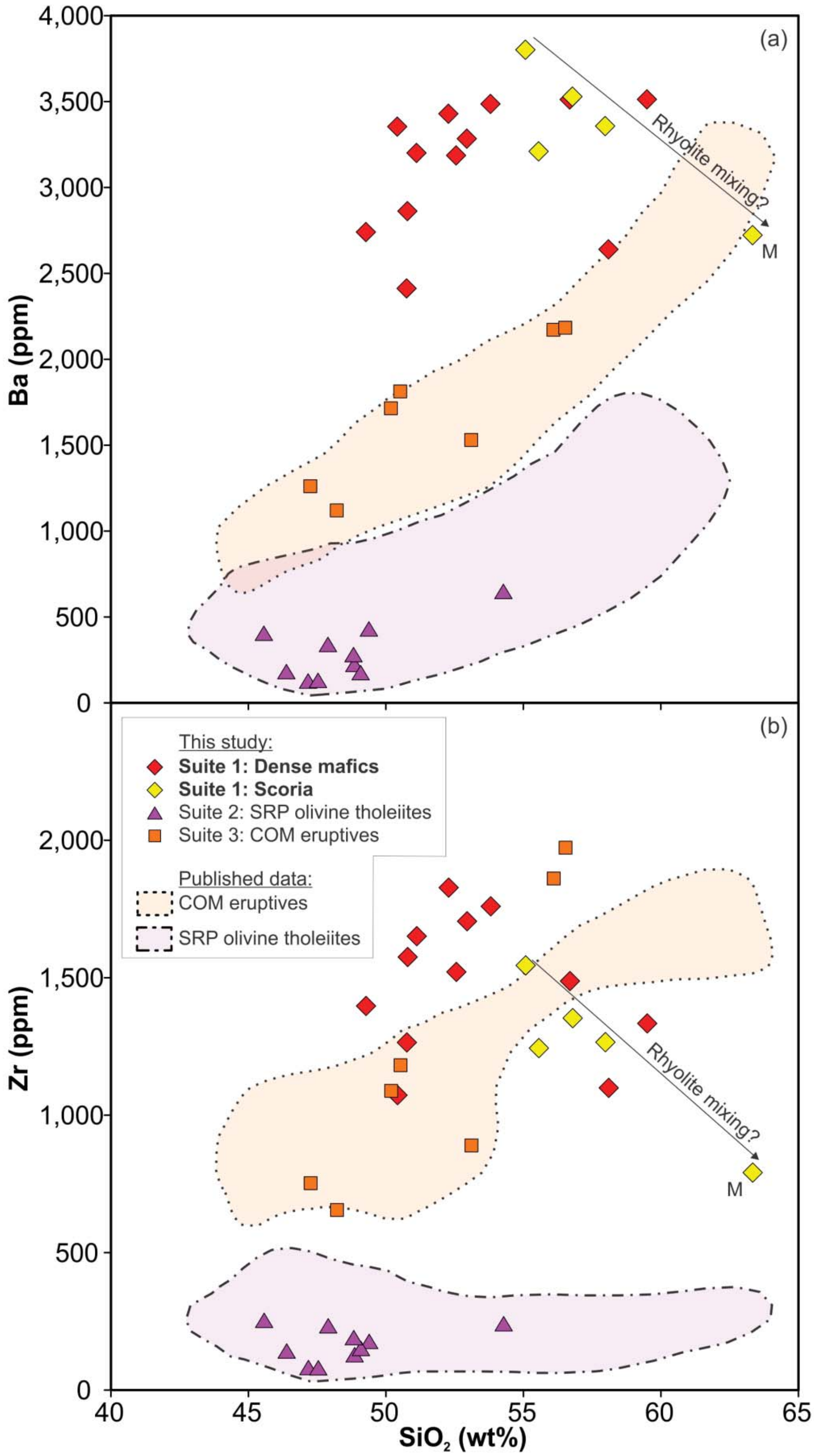

Figure 4

Always consult and cite the final, published document. See http:/www.minsocam.org or GeoscienceWorld

This is a preprint, the final version is subject to change, of the American Mineralogist (MSA)
Cite as Authors (Year) Title. American Mineralogist, in press.
DOI: https://doi.org/10.2138/am-2018-6273

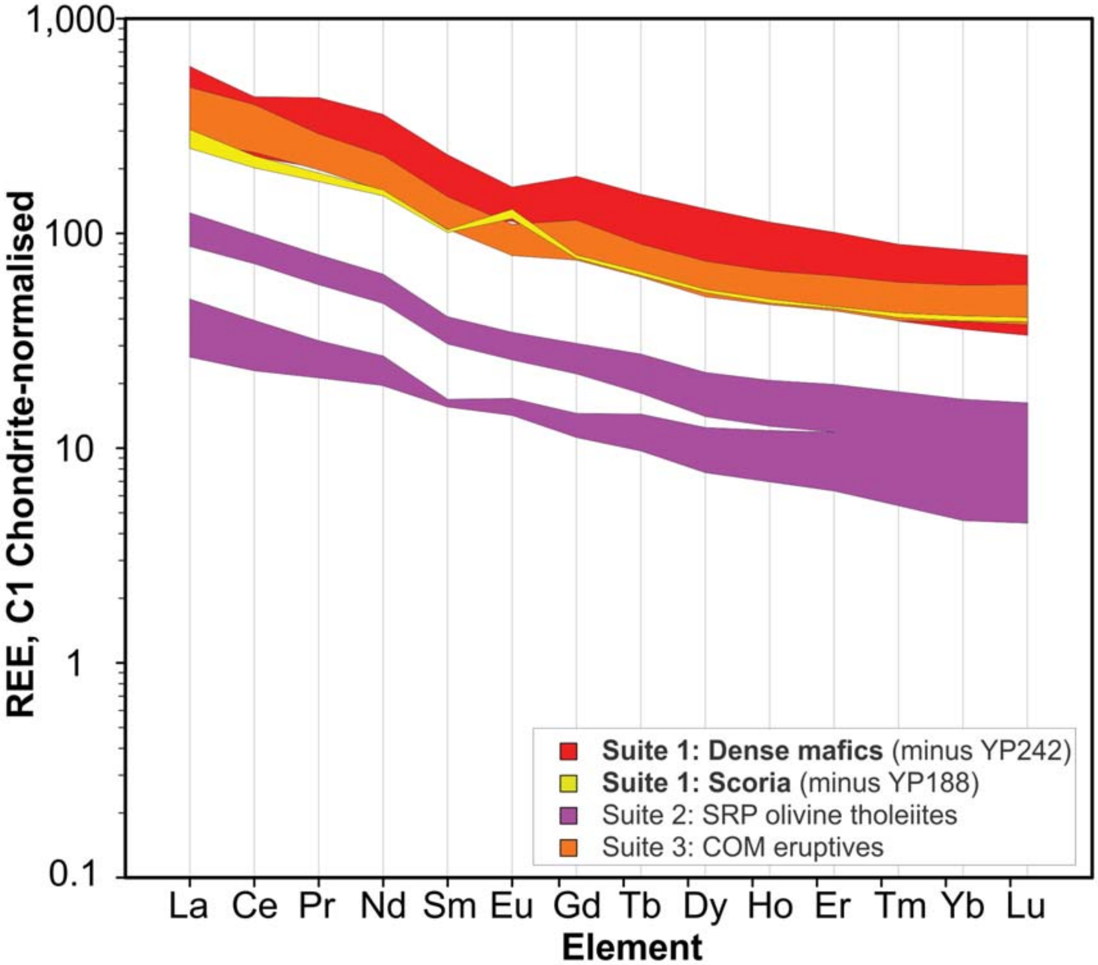

Figure 5

Always consult and cite the final, published document. See http:/www.minsocam.org or GeoscienceWorld

This is a preprint, the final version is subject to change, of the American Mineralogist (MSA)
Cite as Authors (Year) Title. American Mineralogist, in press.
DOI: https://doi.org/10.2138/am-2018-6273

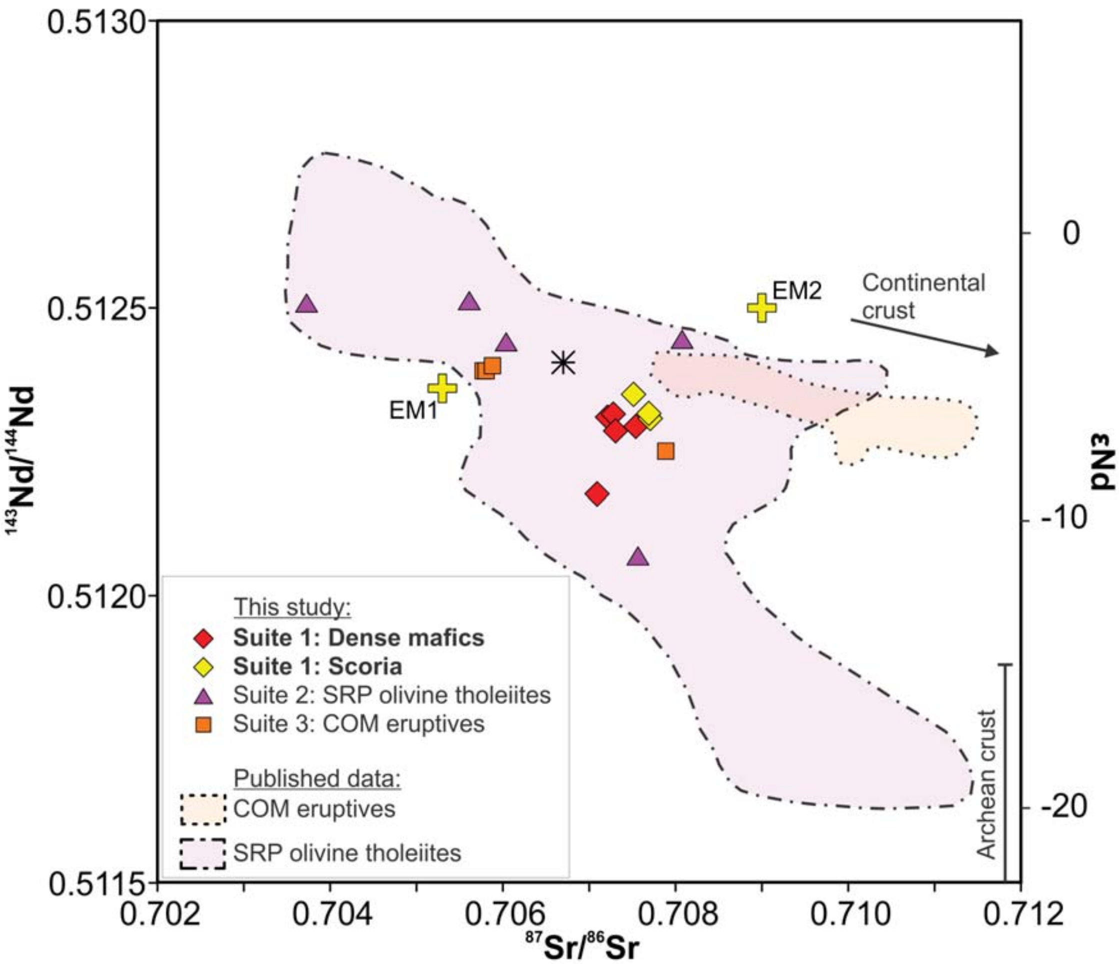

Figure 6

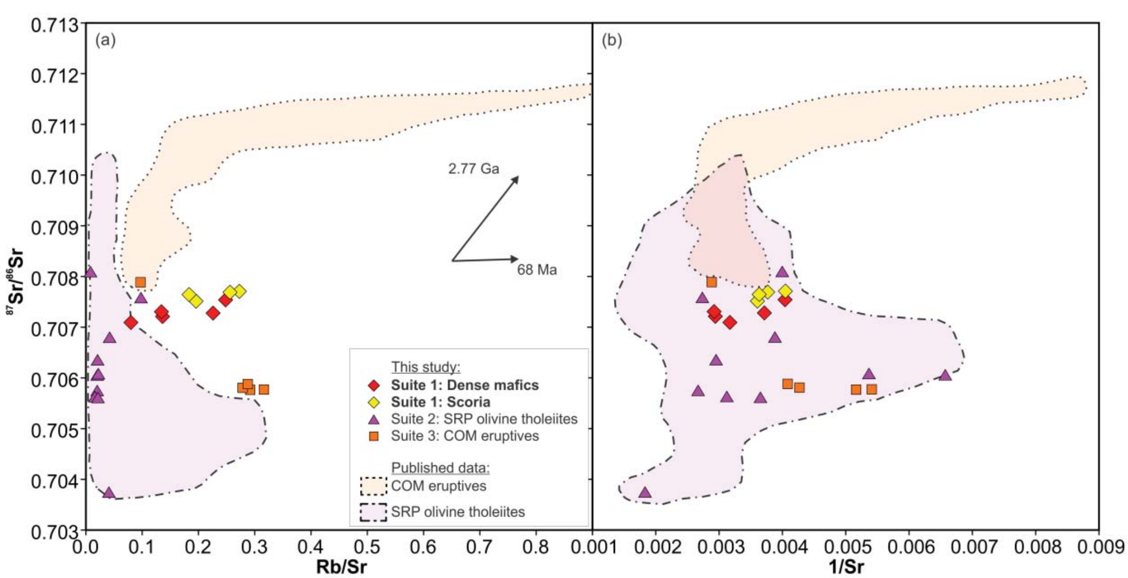

Figure 7

Always consult and cite the final, published document. See http:/www.minsocam.org or GeoscienceWorld

This is a preprint, the final version is subject to change, of the American Mineralogist (MSA)
Cite as Authors (Year) Title. American Mineralogist, in press.
DOI: https://doi.org/10.2138/am-2018-6273

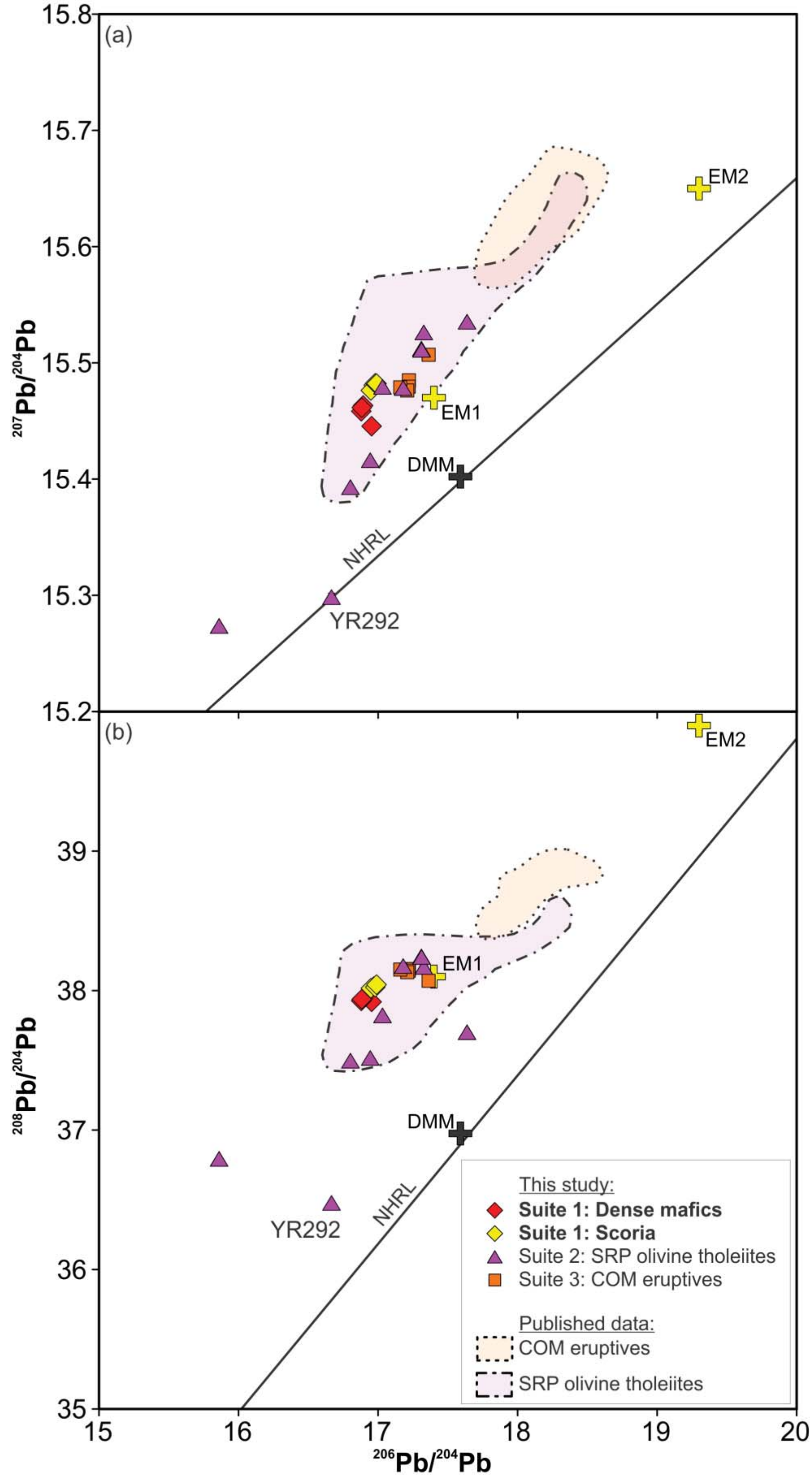

Figure 8

Always consult and cite the final, published document. See http:/www.minsocam.org or GeoscienceWorld

This is a preprint, the final version is subject to change, of the American Mineralogist (MSA)
Cite as Authors (Year) Title. American Mineralogist, in press.
DOI: https://doi.org/10.2138/am-2018-6273

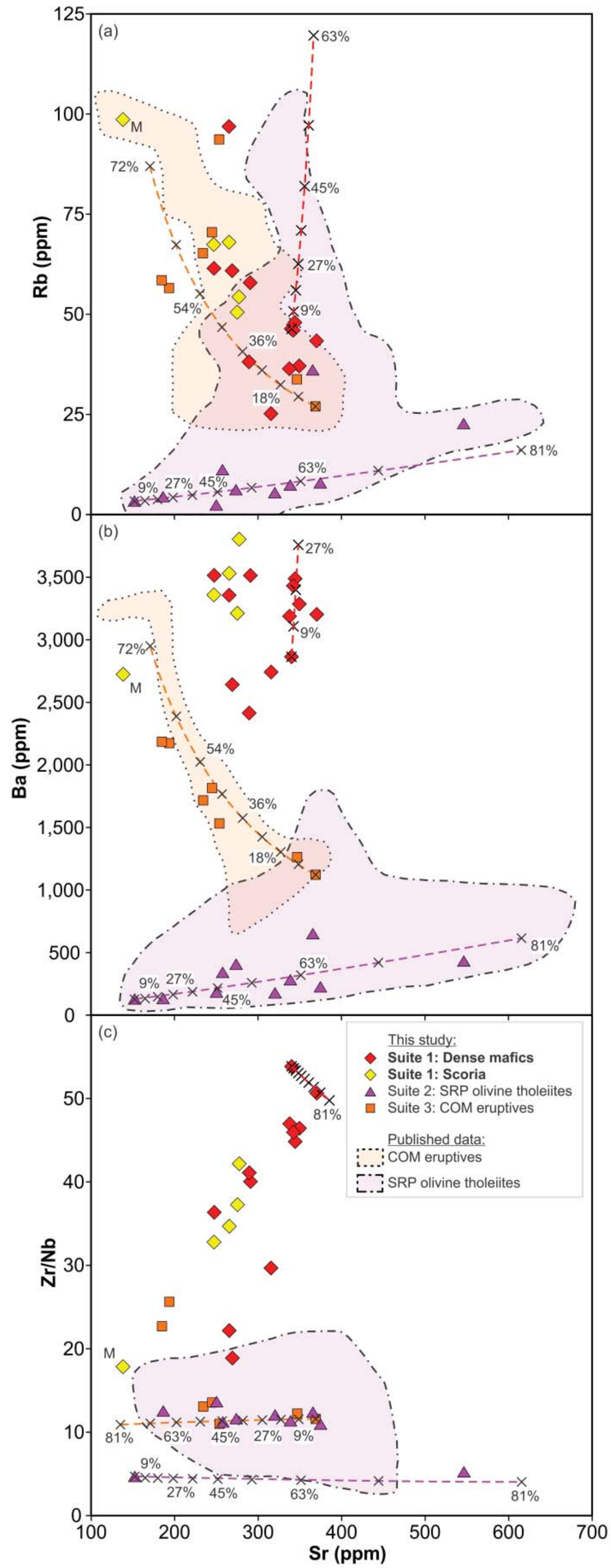

Figure 9

Always consult and cite the final, published document. See http:/www.minsocam.org or GeoscienceWorld

This is a preprint, the final version is subject to change, of the American Mineralogist (MSA)
Cite as Authors (Year) Title. American Mineralogist, in press.
DOI: https://doi.org/10.2138/am-2018-6273

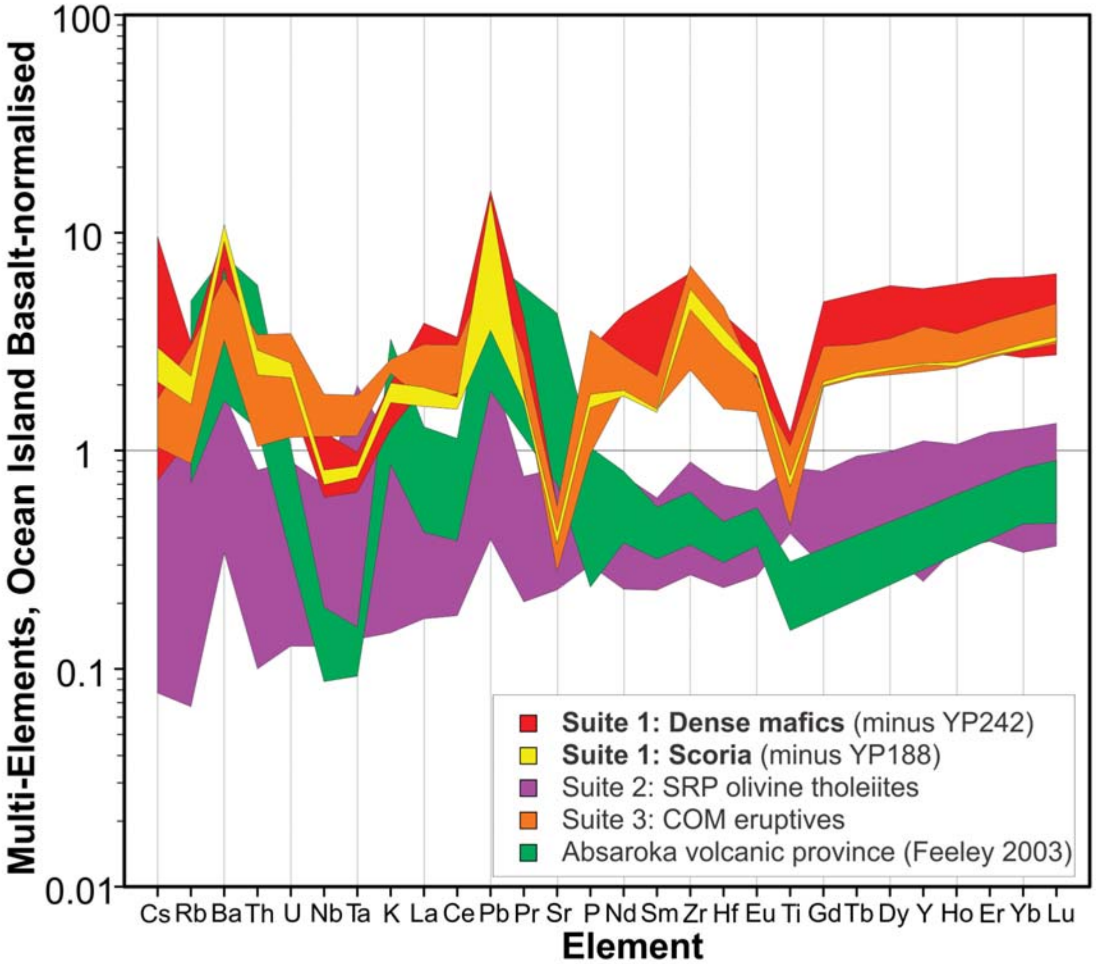

Figure 10

Always consult and cite the final, published document. See http:/www.minsocam.org or GeoscienceWorld

This is a preprint, the final version is subject to change, of the American Mineralogist (MSA)
Cite as Authors (Year) Title. American Mineralogist, in press.
DOI: https://doi.org/10.2138/am-2018-6273

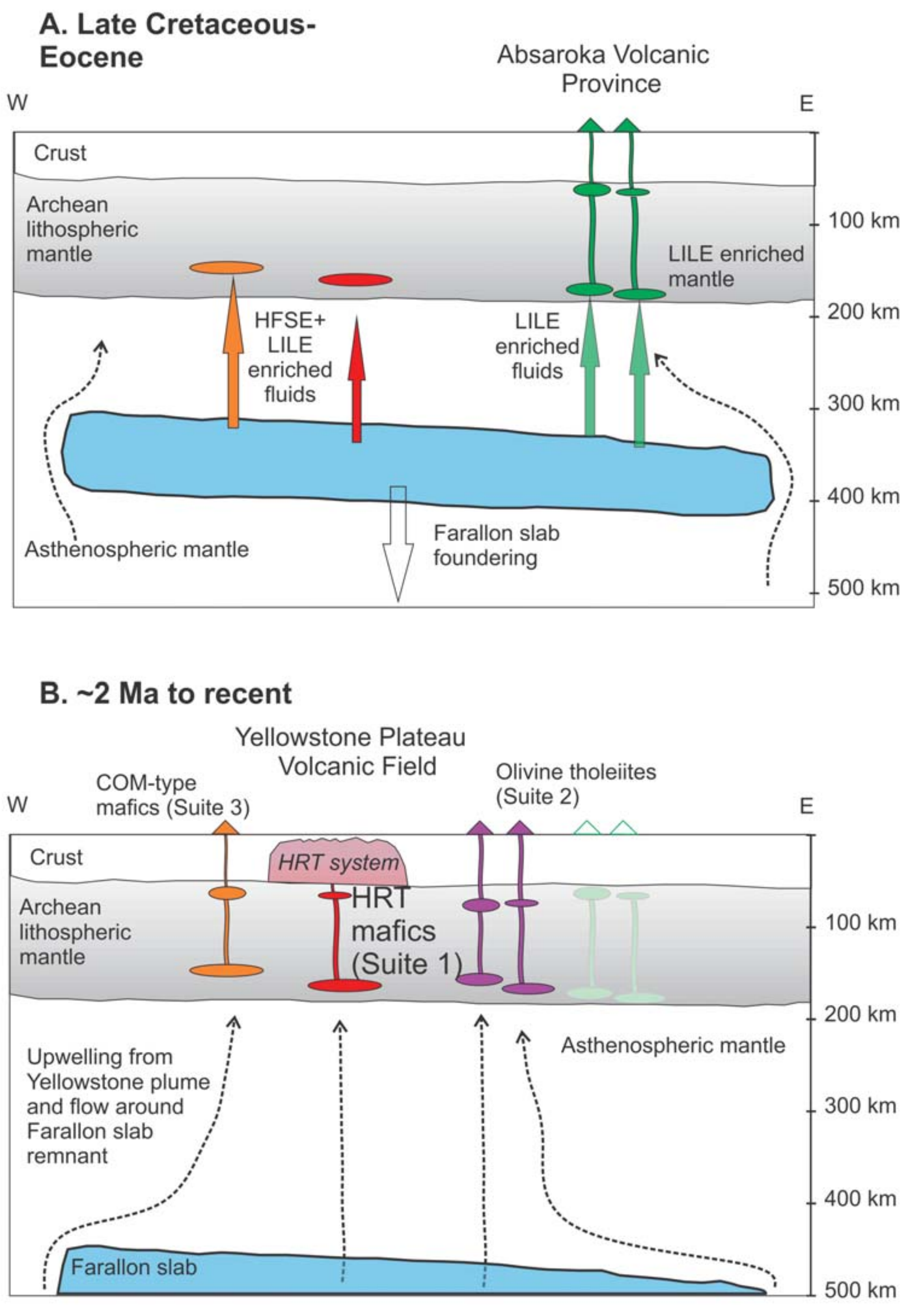

Figure 11

Always consult and cite the final, published document. See http:/www.minsocam.org or GeoscienceWorld